

Working with Stefano: first ideas and later developments

Bryan Webber



UNIVERSITY OF
CAMBRIDGE

- CMW (1991)
- Event shapes (1991-98)
- k_t jet algorithm (1991-94)
- Sudakov shoulder (1997)
- CKKW (2001)

CMW





THE GLUON FORM FACTOR TO HIGHER ORDERS: GLUON-GLUON ANNIHILATION AT SMALL Q_t

S. Catani, E. D'Emilio, L. Trentadue, PL B211 (1988) 335

$$S(Q^2, b^2) = \exp \left[- \int_{b_0^2/b^2}^{Q^2} \frac{dq^2}{q^2} \left(A(\alpha_s(q^2)) \ln \frac{Q^2}{q^2} + B(\alpha_s(q^2)) \right) \right]$$

$$A_g^{(1)} = C_A, \quad A_g^{(2)} = \frac{1}{2} C_A K, \quad B_g^{(1)} = -2\pi\beta_0, \quad \boxed{K = C_A \left(\frac{67}{18} - \frac{1}{6} \pi^2 \right) - \frac{10}{9} T_R N_F}$$

These have to be compared with the previously known [10] coefficients for the quark form factor: $A_q^{(1)} = C_F$, $A_q^{(2)} = \frac{1}{2} C_F K$, $B_q^{(1)} = -\frac{3}{2} C_F$.

J. Kodaira, L. Trentadue, PL B112 (1982) 66

RESUMMATION OF THE QCD PERTURBATIVE SERIES FOR HARD PROCESSES

S. Catani, L. Trentadue, NP B327 (1989) 323

$$\Delta_N(Q^2) = \exp \left[\int_{N_0/N}^1 \frac{dy}{y} \left(2 \int_{yQ^2}^{Q^2} \frac{dk^2}{k^2} A(\alpha_s(yk^2)) + B(\alpha_s(yQ^2)) \right) + O(\alpha_s(\alpha_s \ln N)^n) \right]$$

where the functions $A(\alpha_s)$ and $B(\alpha_s)$ are equal to the ones computed in refs. [9, 10]

QCD COHERENT BRANCHING AND SEMI-INCLUSIVE PROCESSES AT LARGE x

S. Catani, G. Marchesini, B.R. Webber, NP B349 (1991) 635

“In this paper we have studied the ability of the coherent parton branching algorithm, and hence of QCD Monte Carlo programs based on it, to reproduce both the leading and the next-to-leading logarithmic terms in semi-inclusive hard processes such as the DIS and DY processes at large x . ”

“Next-to-leading accuracy will allow one to use Monte Carlo programs to determine $\Lambda_{\overline{\text{MS}}}$, the QCD scale in the $\overline{\text{MS}}$ subtraction scheme, from semi-inclusive data. We find that the same accuracy can be obtained in a program with coherence using only the one-loop splitting functions, provided one uses the two-loop expression for α_s and the following universal relation between $\Lambda_{\overline{\text{MS}}}$ and the scale parameter Λ_{MC} used in the Monte Carlo simulation (for N_f flavours):

$$\Lambda_{\text{MC}} = \exp\left(\frac{67 - 3\pi^2 - 10N_f/3}{2(33 - 2N_f)}\right) \Lambda_{\overline{\text{MS}}}$$
$$\simeq 1.569 \Lambda_{\overline{\text{MS}}} \quad \text{for } N_f = 5. ”$$

- Why is K the same for p_t and threshold resummation?
 - ✦ Not obvious (k_t vs m_t)
 - ✦ Higher orders?
- Casimir scaling?
- Relation to cusp anomalous dimension?

Soft-gluon effective coupling and cusp anomalous dimension

Stefano Catani^(a), Daniel de Florian^(b) and Massimiliano Grazzini^(c)

EPJ C79 (2019) 685

We consider the extension of the CMW soft-gluon effective coupling [1] in the context of soft-gluon resummation for QCD hard-scattering observables beyond the next-to-leading logarithmic accuracy. We present two proposals of a soft-gluon effective coupling that extend the CMW coupling to all perturbative orders in the $\overline{\text{MS}}$ coupling

Soft-gluon effective coupling: perturbative results and the large- n_F limit to all orders

Stefano Catani^(a), Daniel de Florian^(b), Simone Devoto^(c)

Massimiliano Grazzini^(d) and Javier Mazzitelli^(e)

JHEP 11 (2023) 217

- Generalized effective coupling:

$$\tilde{\mathcal{A}}_{\mathcal{F},i}(\alpha_S(\mu^2); \epsilon) = \frac{1}{2} \mu^2 \int_0^\infty dm_T^2 dk_T^2 \delta\left(\mu^2 - \frac{k_T^2}{\mathcal{F}(k_T^2/m_T^2)}\right) w_i(k; \epsilon)$$

$$\hat{w}_i(k; \epsilon) \equiv \frac{1}{2} m_T^4 w_i(k; \epsilon) = \tilde{\mathcal{A}}_{T,i}(\alpha_S(k_T^2); \epsilon) \delta(1-t) + \sum_{n=2}^{+\infty} \left(\frac{\alpha_S(k_T^2)}{\pi}\right)^n [\hat{w}_{T,i}^{(n)}(t; \epsilon)]_+ \quad (t = k_T^2/m_T^2)$$

- All-order universal at conformal point $\epsilon = \beta(\alpha_S)$ (= cusp anom dim)

$$\tilde{\mathcal{A}}_{\mathcal{F}_1,i}(\alpha_S(\mu^2); \epsilon) - \tilde{\mathcal{A}}_{\mathcal{F}_2,i}(\alpha_S(\mu^2); \epsilon) = \sum_{n=2}^{+\infty} \frac{1}{\pi^n} \int_0^1 dt [\alpha_S^n(\mu^2 \mathcal{F}_1(t)) - \alpha_S^n(\mu^2 \mathcal{F}_2(t))] \hat{w}_{T,i}^{(n)}(t; \epsilon)$$

- Universal at 2-loop in 4d:

$$\begin{aligned} \tilde{\mathcal{A}}_{\mathcal{F}_1,i}^{(2)}(\epsilon) - \tilde{\mathcal{A}}_{\mathcal{F}_2,i}^{(2)}(\epsilon) &= \int_0^1 dt [(\mathcal{F}_1(t))^{-2\epsilon} - (\mathcal{F}_2(t))^{-2\epsilon}] \hat{w}_{T,i}^{(2)}(t; \epsilon) \\ &= 2\epsilon \int_0^1 dt \ln \left[\frac{\mathcal{F}_2(t)}{\mathcal{F}_1(t)} \right] \hat{w}_{T,i}^{(2)}(t; \epsilon = 0) + \mathcal{O}(\epsilon^2) \end{aligned}$$

- But not at 3-loop: $\mathcal{A}_{\mathcal{F}_1,i}^{(3)} - \mathcal{A}_{\mathcal{F}_2,i}^{(3)} = 2\pi\beta_0 \int_0^1 dt \ln \left[\frac{\mathcal{F}_2(t)}{\mathcal{F}_1(t)} \right] \hat{w}_{T,i}^{(2)}(t; \epsilon = 0)$

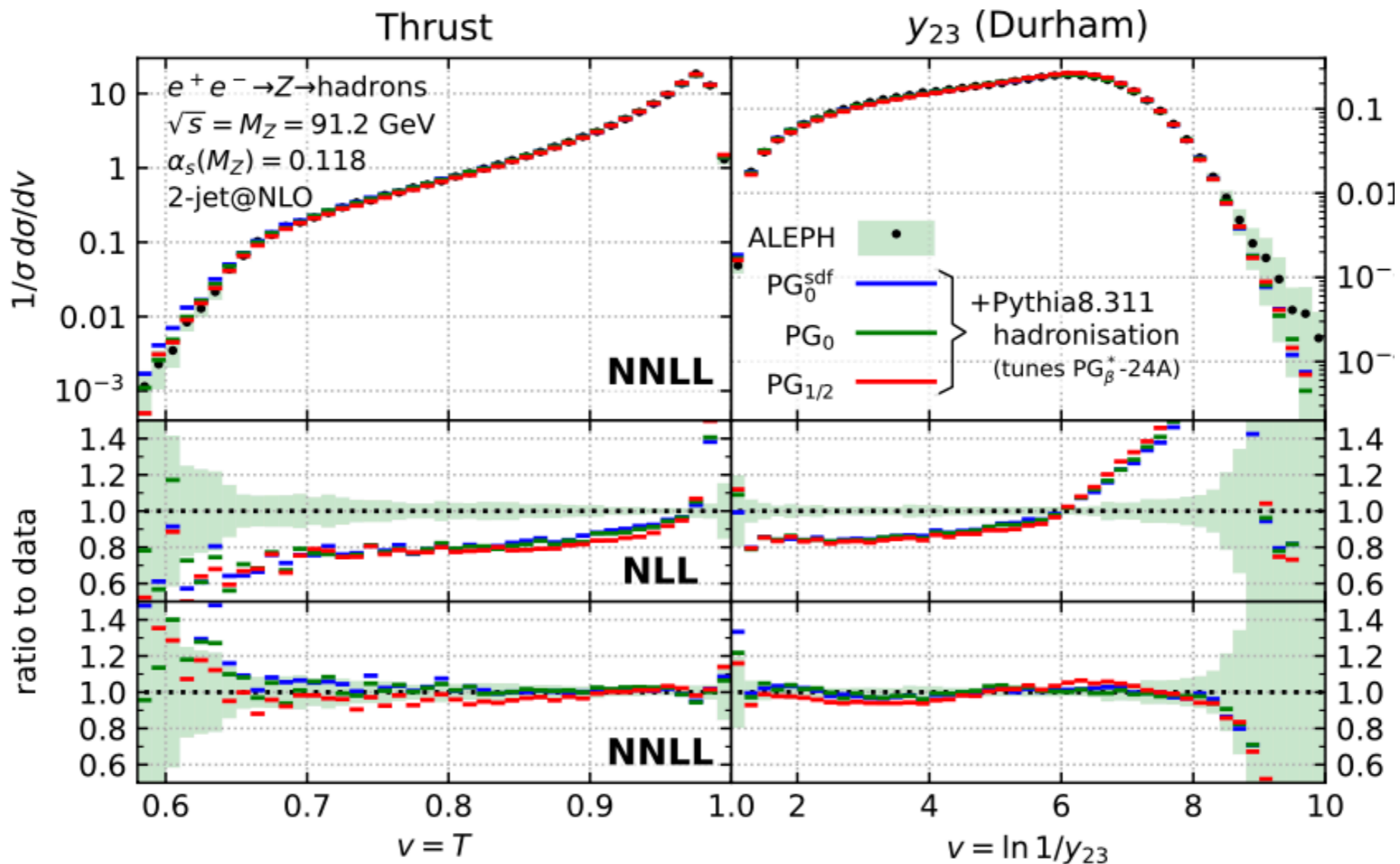
New standard for the logarithmic accuracy of parton showers

Melissa van Beekveld, Mrinal Dasgupta, Basem Kamal El-Menoufi, Silvia Ferrario Ravasio, Keith Hamilton, Jack Helliwell, Alexander Karlberg, Pier Francesco Monni, Gavin P. Salam, Ludovic Scyboz, Alba Soto-Ontoso, and Gregory Soyez

Phys. Rev. Lett. - **Accepted** 5 December, 2024

$$\alpha_{\text{eff}} = \alpha_s \left[1 + \frac{\alpha_s}{2\pi} (K_1 + \Delta K_1(y) + B_2(z)) + \frac{\alpha_s^2}{4\pi^2} K_2 \right],$$

with $\alpha_s \equiv \alpha_s^{\overline{\text{MS}}}(k_t)$ and here the rapidity $y = \ln z/k_t$.



Event Shapes

Event Shapes

- Thrust (CTrTuW, Apr 1991)
- Heavy Jet Mass (CTuW, Aug 1991)
- Jet Broadening (CTuW, Sep 1992)
- General Shapes (CTrTuW, Nov 1992)
- C Parameter (CW, Jan 1998)

Tr=Luca Trentadue, Tu=Graham Turnock

Resummation of large logarithms in e^+e^- event shape distributions

S. Catani, L. Trentadue, G. Turnock, B.R. Webber, NPB 407 (1993) 3

Graham Turnock's recollections of Stefano:

“... an extremely friendly person, who always quickly understood what one was saying and was very open minded and questioning. ... I also remember his white/blackboard was always full of interesting equations and the first thing one wanted to know on entering his room was what he was currently working on. Overall, he was a joy to work with, funny, very inspirational and one of the people in my life I feel most fortunate to have met.”

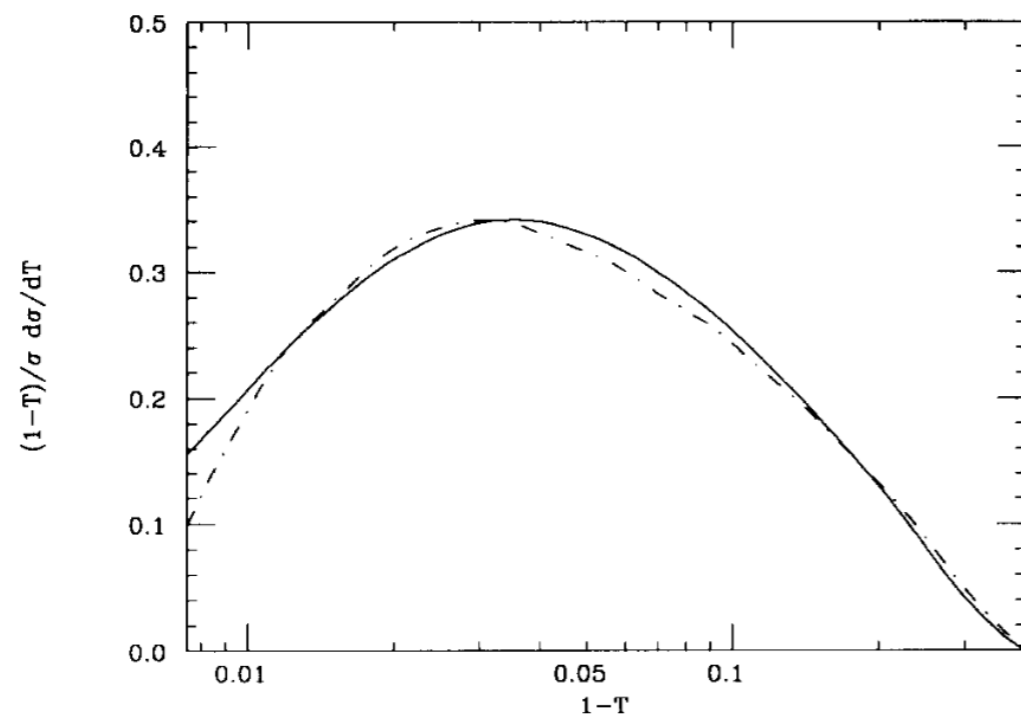


Fig. 8. Comparison between resummed thrust prediction (117) with scale factor $\mu^2/Q^2 = 1$ and $\Lambda_{\overline{\text{MS}}} = 250$ MeV (solid), and fixed-order prediction (98) with scale factor $\mu^2/Q^2 = 0.001$ and $\Lambda_{\overline{\text{MS}}} = 100$ MeV (dot-dashed).

$$R(y) = C(\alpha_S)\Sigma(y, \alpha_S) + D(y, \alpha_S),$$

$$C(\alpha_S) = 1 + \sum_{n=1}^{\infty} C_n \bar{\alpha}_S^n,$$

$$\begin{aligned} \ln \Sigma(y, \alpha_S) &= \sum_{n=1}^{\infty} \sum_{m=1}^{n+1} G_{nm} \bar{\alpha}_S^n L^m \\ &= Lg_1(\alpha_S L) + g_2(\alpha_S L) + \alpha_S g_3(\alpha_S L) + \dots \end{aligned}$$

ALEPH, Phys Rep 294 (1998) I

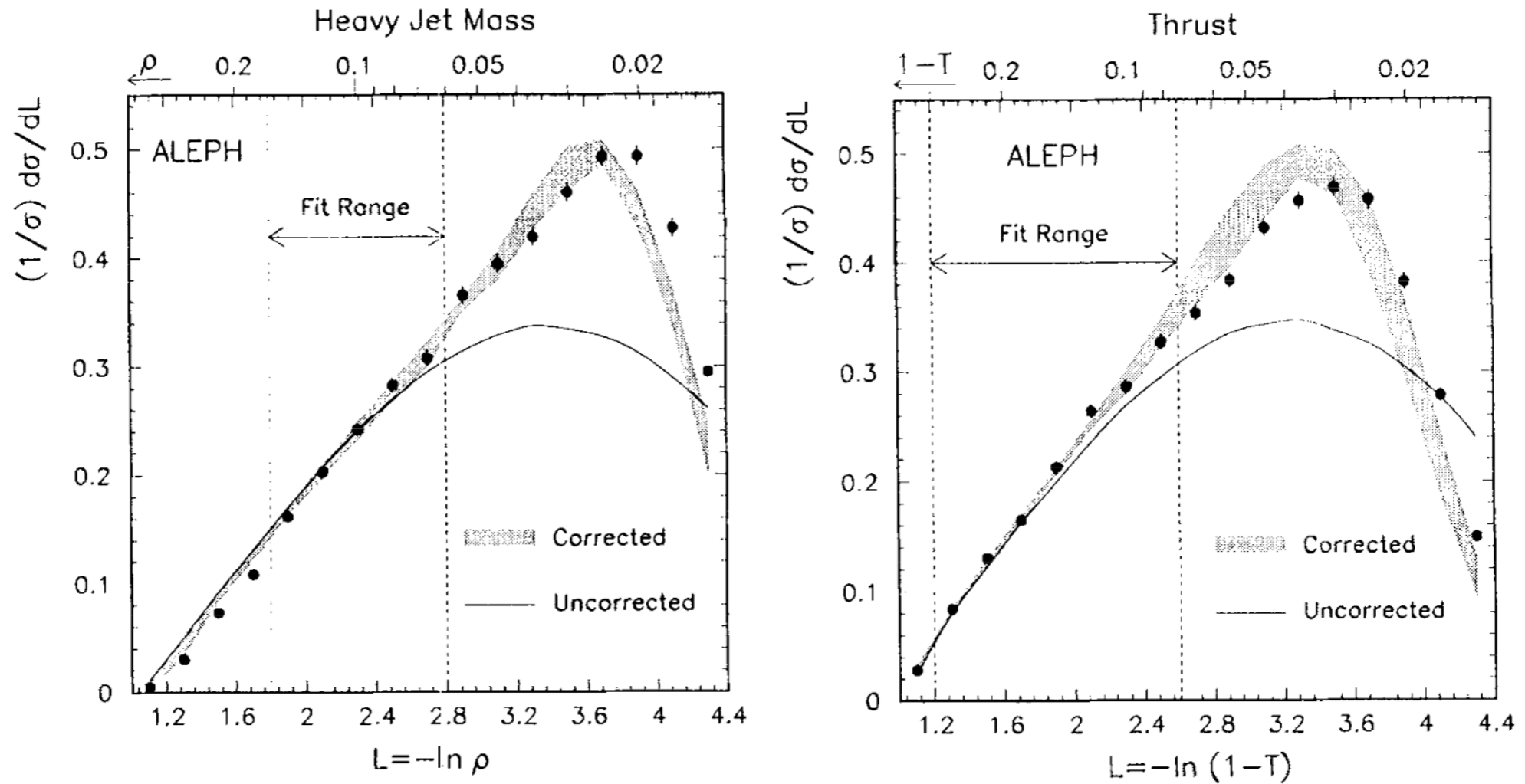


Fig. 24. Experimental distributions (statistical errors only) together with bands covering the predictions using the three hadronization models and the central values of α_s for $\mu = M_Z$ and R matching. The curves are the predictions for the same values of α_s without hadronization corrections.

$$\alpha_s(M_Z)|_T = 0.1263 \pm 0.0008_{\text{stat}} \pm 0.0010_{\text{syst}} \pm 0.0028_{\text{hadr}} \pm 0.0065_{\text{theo}}$$

$$\alpha_s(M_Z)|_\rho = 0.1243 \pm 0.0010_{\text{stat}} \pm 0.0033_{\text{syst}} \pm 0.0042_{\text{hadr}} \pm 0.0057_{\text{theo}}$$

“The theoretical uncertainty covers the uncertainty due to the choice of matching scheme as well as the variation of the renormalization scale used in the calculation in the range $-1 \leq \ln \mu^2/s \leq +1$. The central values are given at $\mu^2 = s$. In contrast with most analyses using second order QCD, this analysis using resummed predictions does not prefer values of μ much smaller than the centre-of-mass energy.”

Log-R Matching: NNLO+NLLA

$$\begin{aligned} \ln R(y) = & Lg_1(\alpha_S L) + g_2(\alpha_S L) + \bar{\alpha}_S(R_1(y) - G_{11}L - G_{12}L^2) \\ & + \bar{\alpha}_S^2(R_2(y) - \frac{1}{2}[R_1(y)]^2 - G_{22}L^2 - G_{23}L^3) \\ & + \bar{\alpha}_S^3\{R_3(y) - R_1(y)R_2(y) + \frac{1}{3}[R_1(y)]^3 - G_{33}L^3 - G_{34}L^4\} \end{aligned}$$

S. Catani et al. / Resummation of large logs in e^+e^- (T, M_H, C)

TABLE 1

Logarithmic coefficients G_{nm} for thrust; $\zeta(3) = 1.202057\dots$

G_{11}	=	$+3C_F$
G_{12}	=	$-2C_F$
G_{22}	=	$-C_F[48\pi^2C_F + (169 - 12\pi^2)C_A - 22N_f]/36$
G_{23}	=	$-C_F(11C_A - 2N_f)/3$
G_{33}	=	$+C_F[2304\zeta(3)C_F^2 - 792\pi^2C_FC_A - (3197 - 132\pi^2)C_A^2$ $+ (108 + 144\pi^2)C_FN_f + (1024 - 24\pi^2)C_AN_f - 68N_f^2]/108$
G_{34}	=	$-7C_F(11C_A - 2N_f)^2/108$

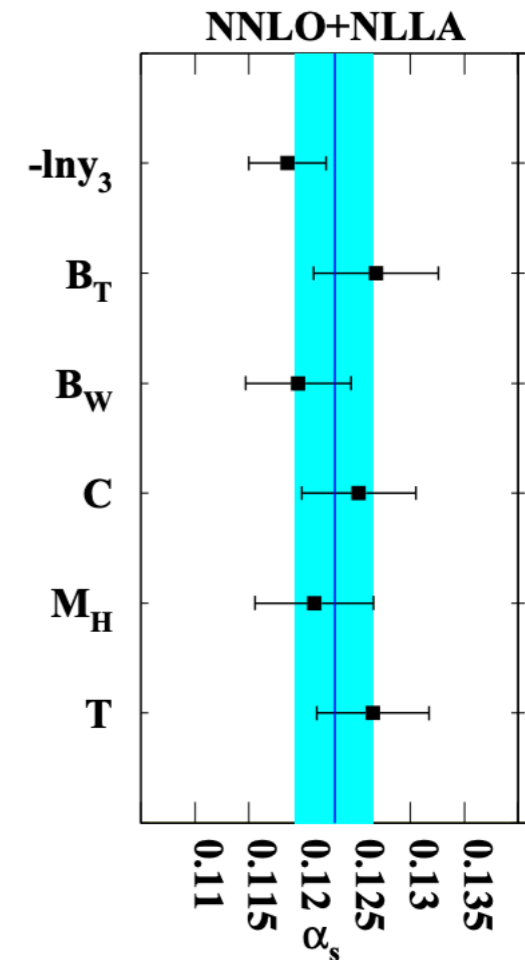
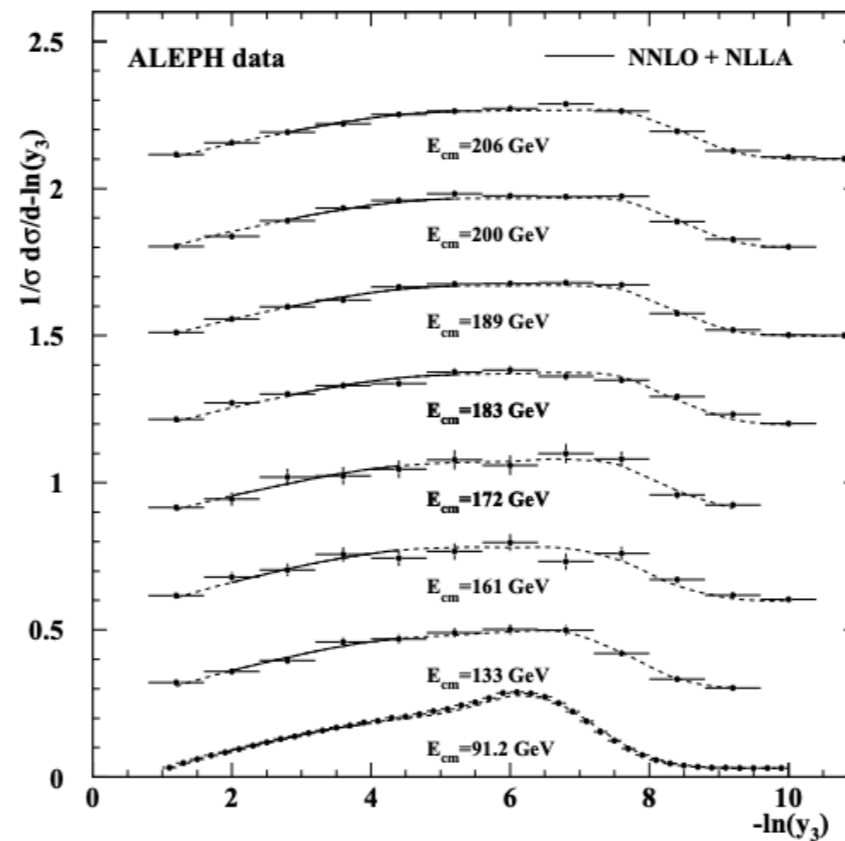
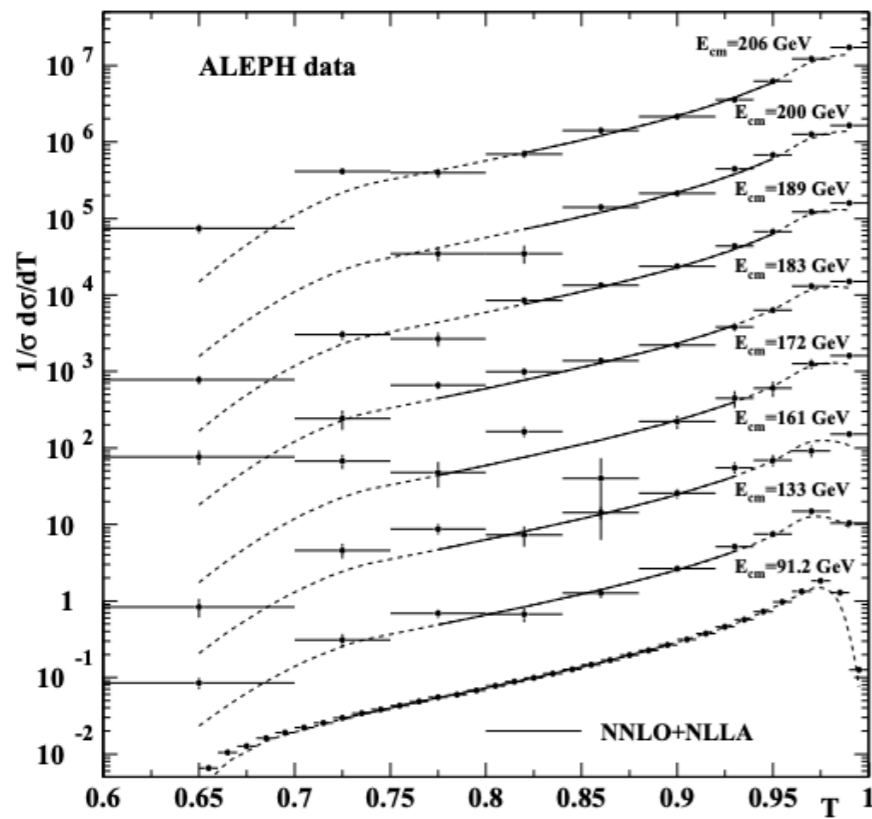
+ T. Gehrmann, G. Luisoni, H. Stenzel, PLB 664 (2008) 265 (B_T, B_W, y₃)

Determination of the strong coupling constant using matched NNLO+NLLA predictions for hadronic event shapes in e^+e^- annihilations

G. Dissertori,^a A. Gehrmann-De Ridder,^a T. Gehrmann,^b E.W.N. Glover,^c
G. Heinrich,^c G. Luisoni,^b and H. Stenzel,^d JHEP 08 (2009) 036

$$\alpha_s(M_Z) = 0.1224 \pm 0.0009 (\text{stat}) \pm 0.0009 (\text{exp}) \pm 0.0012 (\text{had}) \pm 0.0035 (\text{theo})$$

• JHEP 08 (2009) 036



K_T Algorithm

Jet cross sections at leading double logarithm in e^+e^- annihilation

N. Brown, W.J. Stirling, PLB 252 (1990) 657

Received 17 August 1990; revised manuscript received 8 October 1990

- **JADE algorithm:** $y_{ij}^J = 2E_i E_j (1 - \cos \theta_{ij}) / Q^2 \simeq m_{ij}^2 / Q^2$
- ✿ **Combine if** $y_{ij}^J < y_{\text{cut}}$

- **Jet rates:** $L = \ln(1/y_{\text{cut}})$

$y_{gg}^J < y_{qg}^J, y_{\bar{q}g}^J$

$$R_2^J = 1 - \frac{C_F \alpha_S}{\pi} L^2 + \frac{5}{6} \frac{1}{2!} \left(\frac{C_F \alpha_S}{\pi} L^2 \right)^2 + ???$$

$$R_3^J = \frac{C_F \alpha_S}{\pi} L^2 - \frac{19}{12} \frac{1}{2!} \left(\frac{C_F \alpha_S}{\pi} L^2 \right)^2 + ???$$

$$R_4^J = \frac{3}{4} \frac{1}{2!} \left(\frac{C_F \alpha_S}{\pi} L^2 \right)^2 + ???$$

Workshop on Jet Studies at LEP and HERA, Durham, UK, December 1990

(Comment by Yuri Dokshitzer)

- **k_t algorithm:** $y_{ij} = 2 \min\{E_i^2, E_j^2\}(1 - \cos \theta_{ij})/Q^2 \simeq k_t^2/Q^2$

- ✦ **Combine if** $y_{ij} < y_{\text{cut}}$

- **Jet rates:** $L = \ln(1/y_{\text{cut}})$

$$R_2 = \exp\left(-\frac{C_F \alpha_S}{2\pi} L^2 + \dots\right)$$

$$R_{n+2} = \frac{1}{n!} \left(\frac{C_F \alpha_S}{2\pi} L^2\right)^n + \dots$$

Graham Turnock:

“In terms of particular incidents, one that sticks in my mind was the time you, me, Stefano and Yuri went one evening to one of our rooms at the Durham conference and invented the k_t algorithm. I remember Stefano being on particularly creative form on that occasion.”

New clustering algorithm for multijet cross sections in e^+e^- annihilation

S. Catani, Yu.L. Dokshitzer, M.Olsson, G. Turnock, B.R. Webber, PLB 269 (1991) 432

$$R_n^Z = \frac{1}{n!} \left. \frac{d^n \phi_Z}{du^n} \right|_{u=0}, \quad \phi_Z = \phi_q^2$$

$$\phi_q(u, Q) = u \Delta_q(Q) \exp \left(\int_{Q_0}^Q dq \Gamma_q(Q, q) \phi_g(u, q) \right), \quad Q_0 = Q \sqrt{y}_{\text{cut}}$$

$$\phi_g(u, Q) = u \Delta_g(Q) \exp \left(\int_{Q_0}^Q dq \left[\Gamma_g(Q, q) \phi_g(u, q) + \Gamma_f(q) \frac{\phi_q(u, q)^2}{\phi_g(u, q)} \right] \right)$$

$$\Delta_q(Q) = \exp \left(- \int_{Q_0}^Q dq \Gamma_q(Q, q) \right),$$

$$\Delta_g(Q) = \exp \left(- \int_{Q_0}^Q dq [\Gamma_g(Q, q) + \Gamma_f(q)] \right)$$

$$\Gamma_q(Q, q) = \frac{2C_F}{\pi} \frac{\alpha_s(q^2)}{q} \left(\ln \frac{Q}{q} - \frac{3}{4} \right),$$

$$\Gamma_g(Q, q) = \frac{2C_A}{\pi} \frac{\alpha_s(q^2)}{q} \left(\ln \frac{Q}{q} - \frac{11}{12} \right), \quad \Gamma_f(q) = \frac{n_f}{3\pi}.$$

“ It is a pleasure to thank S. Bethke, G. Marchesini, P. Nason, W.J. Stirling, D.E. Soper and L. Trentadue for discussions and correspondence on this topic. We would especially like to acknowledge many valuable and stimulating conversations with Nick Brown, to whose memory we respectfully dedicate this paper.”

Jet Rates to $\mathcal{O}(\alpha_S^2)$

$$R_2^Z = 1 + \frac{1}{2}a(3C_F L - C_F L^2) + \frac{1}{144}a^2(99C_A C_F L^2 + 162C_F^2 L^2 - 44C_A C_F L^3 - 108C_F^2 L^3 + 18C_F^2 L^4 - 18C_F L^2 n_f + 8C_F L^3 n_f),$$

$$R_3^Z = \frac{1}{2}a(-3C_F L + C_F L^2) + \frac{1}{48}a^2(-66C_A C_F L^2 - 108C_F^2 L^2 + 28C_A C_F L^3 + 72C_F^2 L^3 - C_A C_F L^4 - 12C_F^2 L^4 + 12C_F L^2 n_f - 4C_F L^3 n_f),$$

$$R_4^Z = \frac{1}{144}a^2(99C_A C_F L^2 + 162C_F^2 L^2 - 40C_A C_F L^3 - 108C_F^2 L^3 + 3C_A C_F L^4 + 18C_F^2 L^4 - 18C_F L^2 n_f + 4C_F L^3 n_f). \quad (a = \alpha_S(Q)/\pi)$$

$$R_n^H = \frac{1}{n!} \left. \frac{d^n \phi_H}{du^n} \right|_{u=0}, \quad \phi_H = \phi_g^2$$

$$R_2^H = 1 + \frac{1}{6}a(11C_A L - 3C_A L^2 - 2L n_f) + \frac{1}{144}a^2(363C_A^2 L^2 - 176C_A^2 L^3 + 18C_A^2 L^4 - 132C_A L^2 n_f + 32C_A L^3 n_f + 12L^2 n_f^2),$$

$$R_3^H = \frac{1}{6}a(-11C_A L + 3C_A L^2 + 2L n_f) + \frac{1}{144}a^2(-726C_A^2 L^2 + 352C_A^2 L^3 - 39C_A^2 L^4 + 220C_A L^2 n_f + 36C_F L^2 n_f - 56C_A L^3 n_f - 8C_F L^3 n_f - 16L^2 n_f^2),$$

$$R_4^H = \frac{1}{144}a^2(363C_A^2 L^2 - 176C_A^2 L^3 + 21C_A^2 L^4 - 88C_A L^2 n_f - 36C_F L^2 n_f + 24C_A L^3 n_f + 8C_F L^3 n_f + 4L^2 n_f^2).$$

$$R_n^Z = (aL^2)^{n-2} (A + B/L + C/L^2)$$

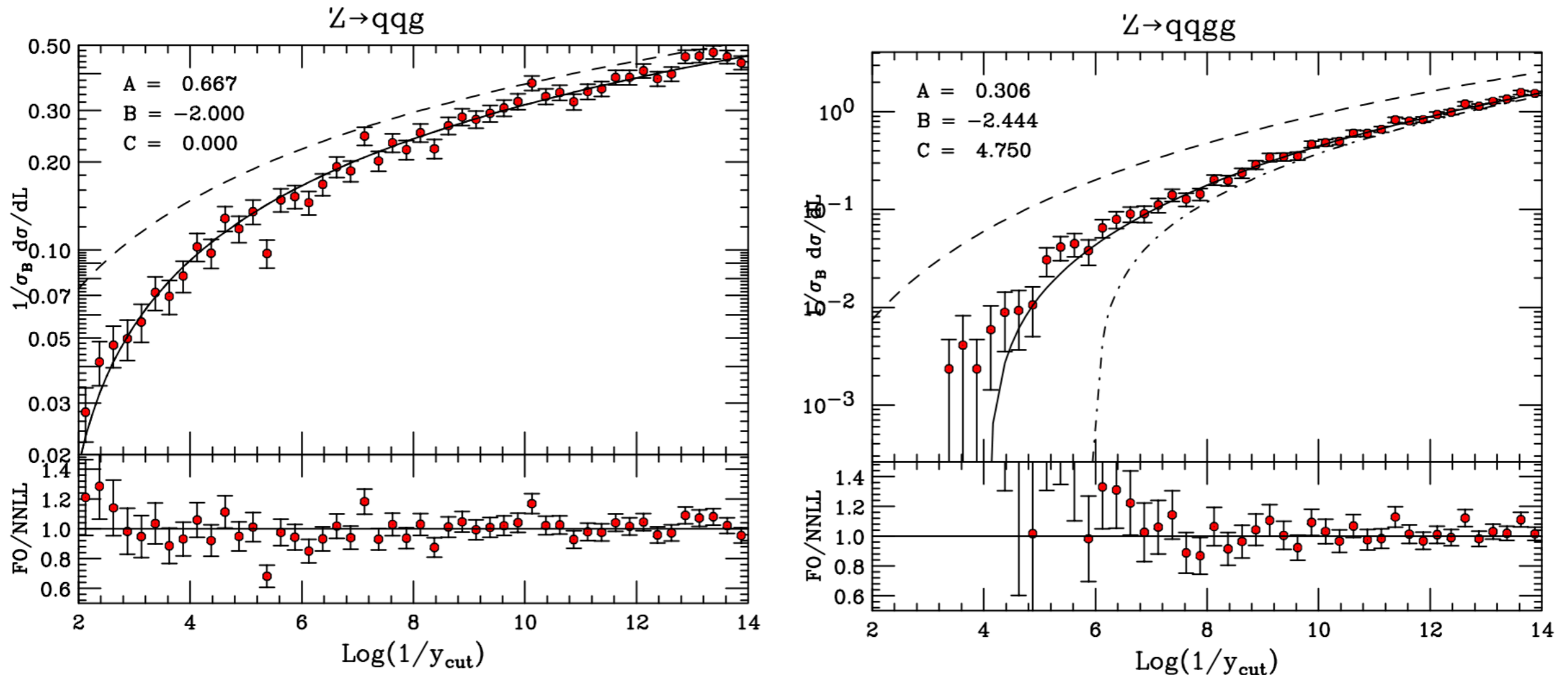


Figure 4: Differential distribution of $L = \ln(1/y_{\text{cut}})$ in $Z^0 \rightarrow d\bar{d} + 1$ and 2 gluons. Points are MadGraph data using leading-order exact matrix elements. Dashed, dot-dashed and solid curves show the leading-log, NLL and NNLL results, respectively.

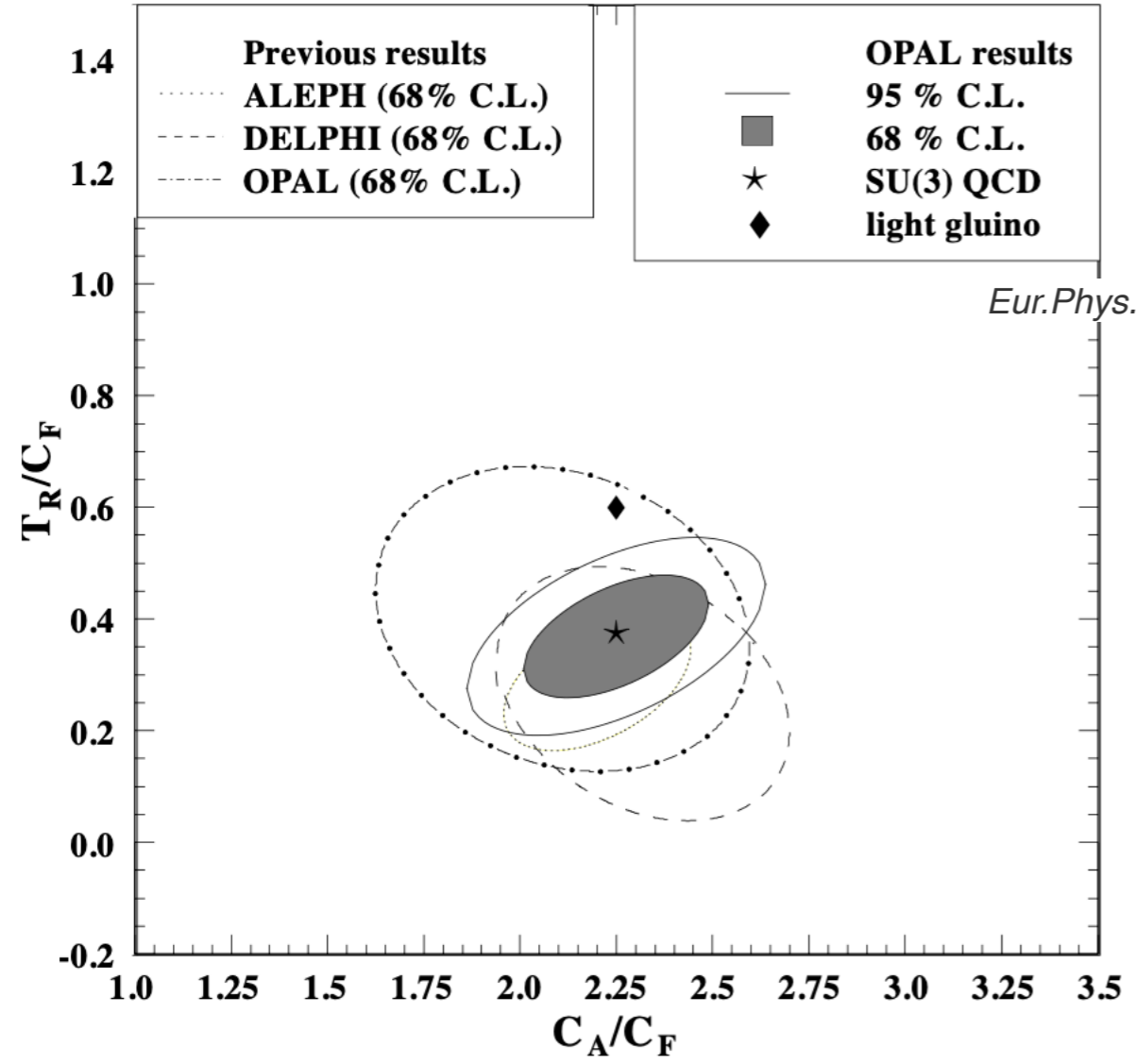
(BRW, unpublished)

A Simultaneous Measurement of the QCD Colour

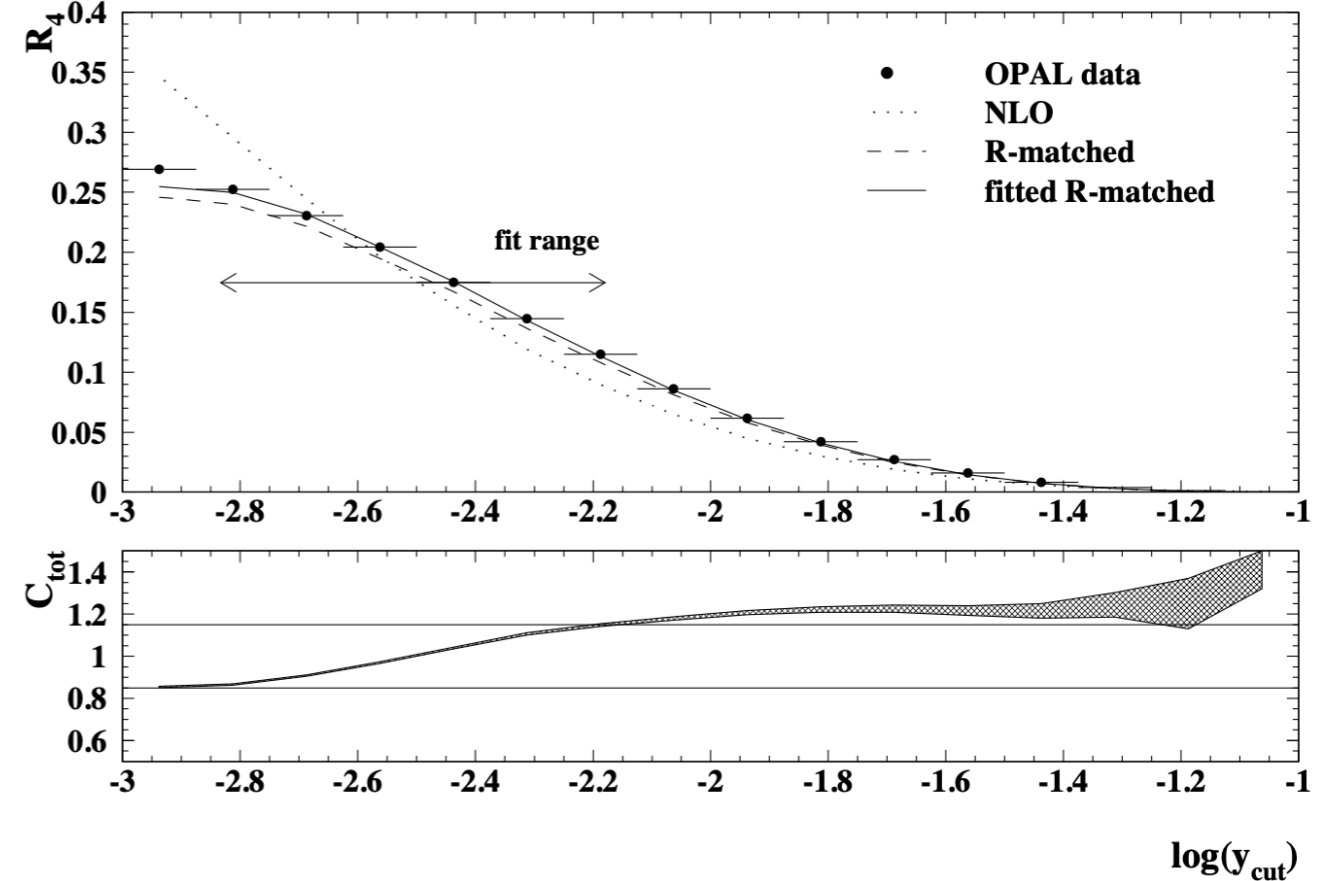
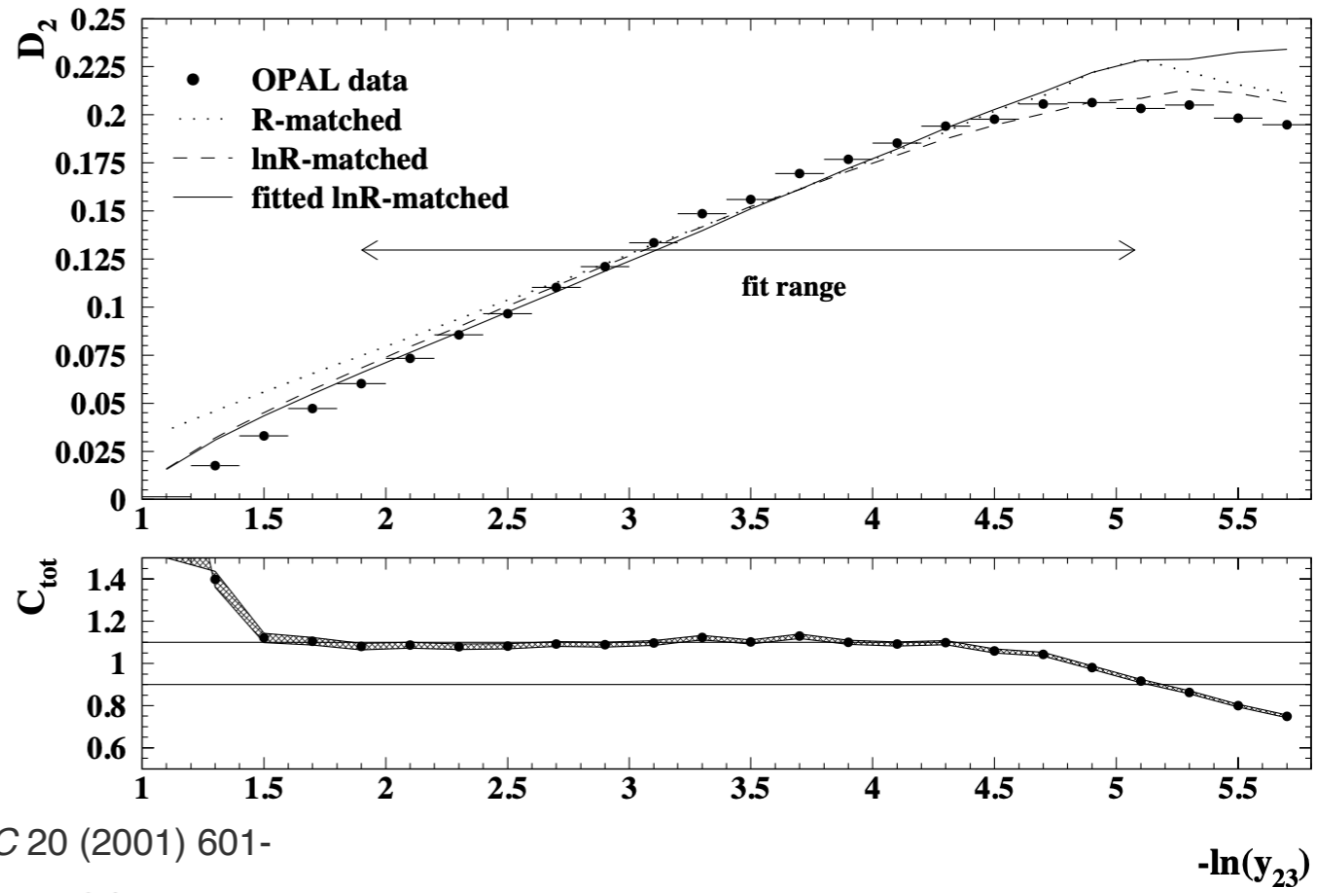
Factors and the Strong Coupling

OPAL, EPJC 20 (2001) 601

$$\alpha_s(M_Z) = 0.120 \pm 0.011(\text{stat.}) \pm 0.020(\text{syst.})$$



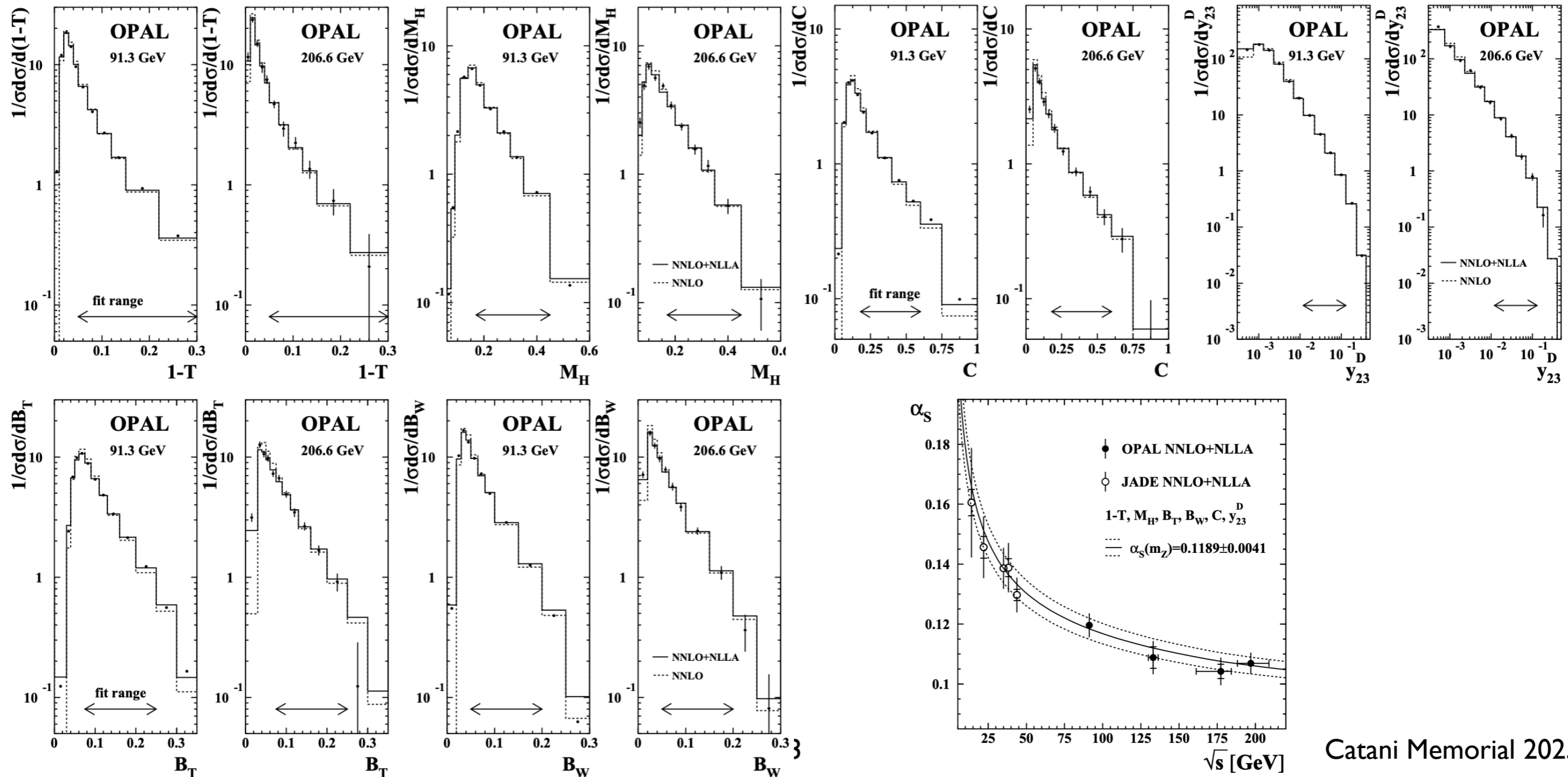
Eur.Phys.J.C 20 (2001) 601-



Determination of α_S using OPAL hadronic event shapes at $\sqrt{s} = 91 - 209$ GeV and resummed NNLO calculations

OPAL, EPJC 71 (2011) 1733

$$\alpha_S(m_{Z^0}) = 0.1189 \pm 0.0008(\text{stat.}) \pm 0.0016(\text{exp.}) \pm 0.0010(\text{had.}) \pm 0.0036(\text{theo.}).$$



Longitudinally-invariant k_{\perp} -clustering algorithms for hadron–hadron collisions

S. Catani, Yu.L. Dokshitzer, M.H. Seymour, B.R. Webber, NPB 406 (1993) 187

Received 9 March 1993

Accepted for publication 5 April 1993

$$d_{kB} = p_{tk}^2, \quad d_{kl} = \min(p_{tk}^2, p_{tl}^2) R_{kl}^2,$$
$$R_{kl}^2 = (\eta_k - \eta_l)^2 + (\phi_k - \phi_l)^2.$$

Successive Combination Jet Algorithm For Hadron Collisions

S.D. Ellis, D.E. Soper, PRD 48 (1993)

Received 29 April 1993

$$d_{ij} = \min(E_{T,i}^2, E_{T,j}^2) [(\eta_i - \eta_j)^2 + (\phi_i - \phi_j)^2] / R^2.$$

[ICHEP 92, Dallas, Texas, USA, August, 1992 ...]

The Inclusive Jet Cross Section in $p\bar{p}$ Collisions at $\sqrt{s} = 1.8$ TeV using the k_{\perp} Algorithm

Subjet Multiplicity of Gluon and Quark Jets Reconstructed with the k_{\perp} Algorithm in $p\bar{p}$ Collisions

DØ Collaboration, PLB 25 (2002) 211, PRD 65 (2002) 052008

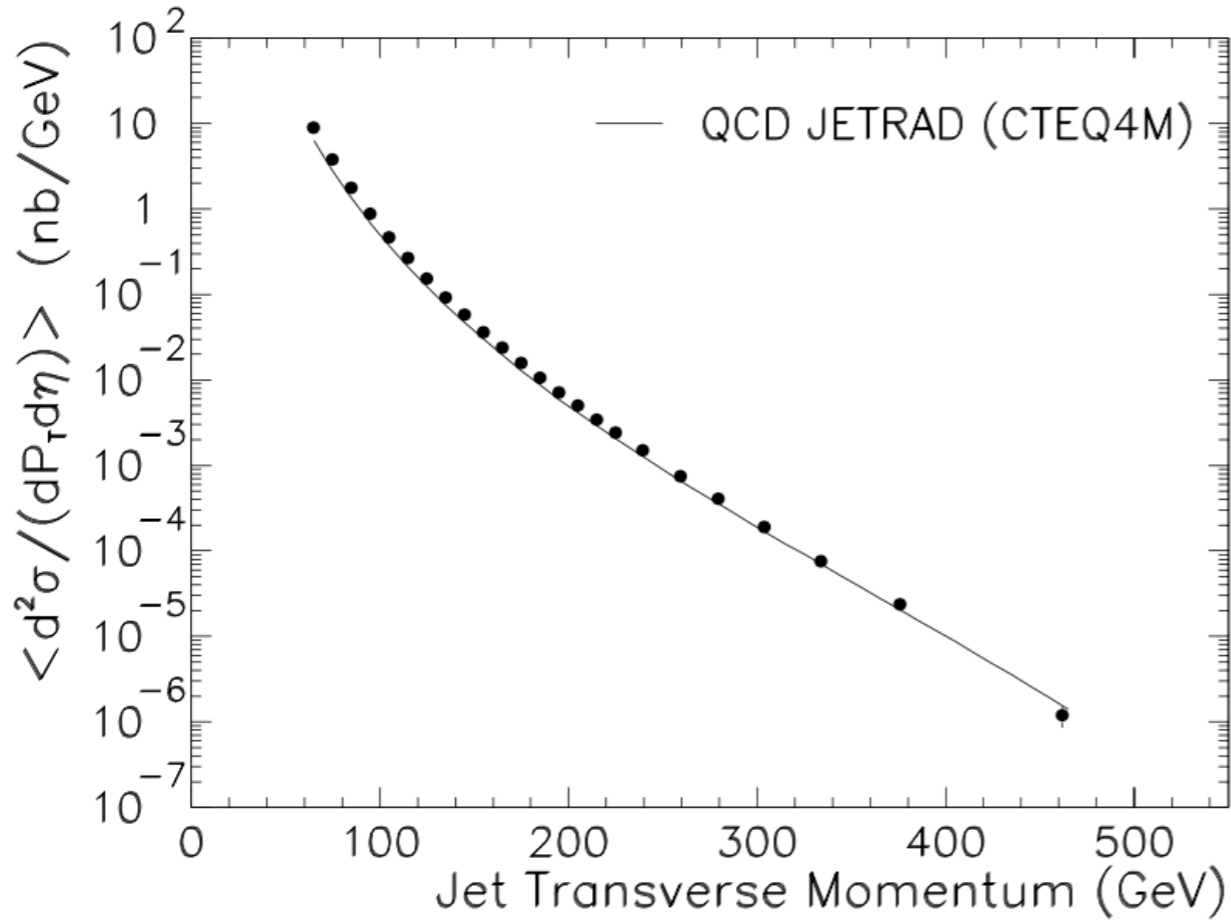


FIG. 1. The central ($|\eta| < 0.5$) inclusive jet cross section obtained with the k_{\perp} algorithm at $\sqrt{s} = 1.8$ TeV. Only statistical errors are included. The solid line shows a prediction from NLO pQCD.

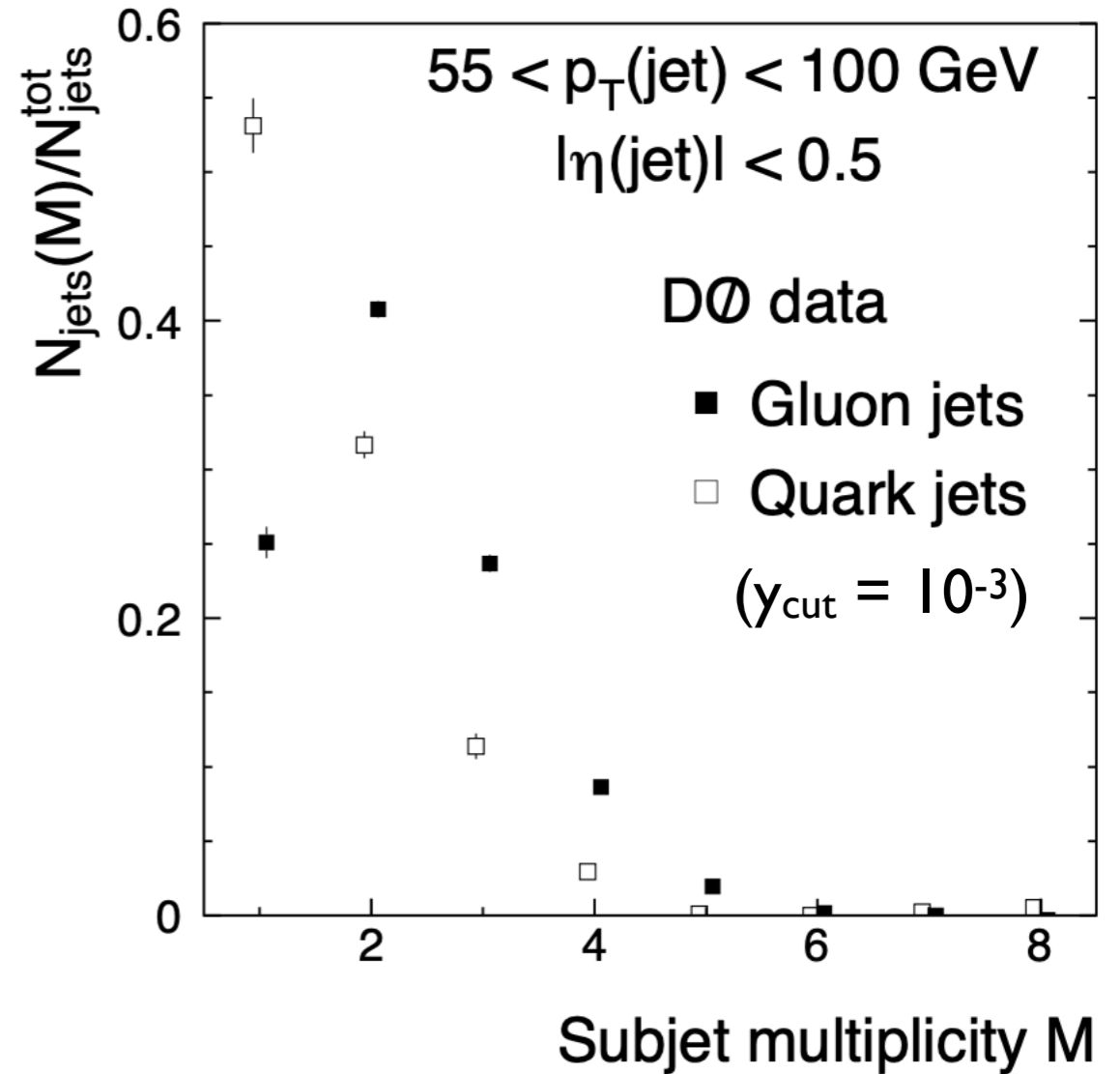
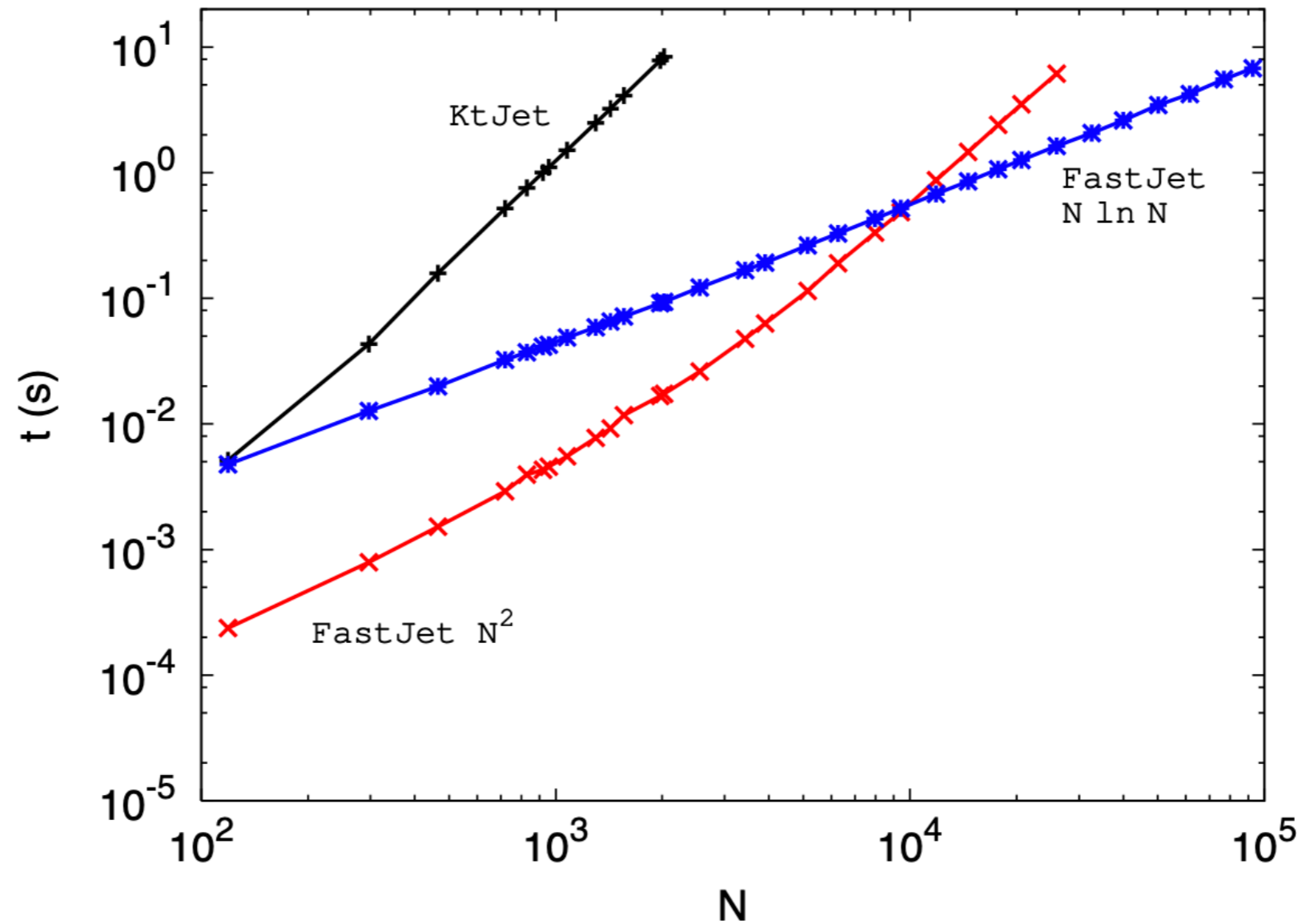


FIG. 29. Corrected subjet multiplicity for gluon and quark jets, extracted from DØ data.

Dispelling the N^3 myth for the k_t jet-finder

Matteo Cacciari, Gavin P. Salam, PLB 641 (2006) 57

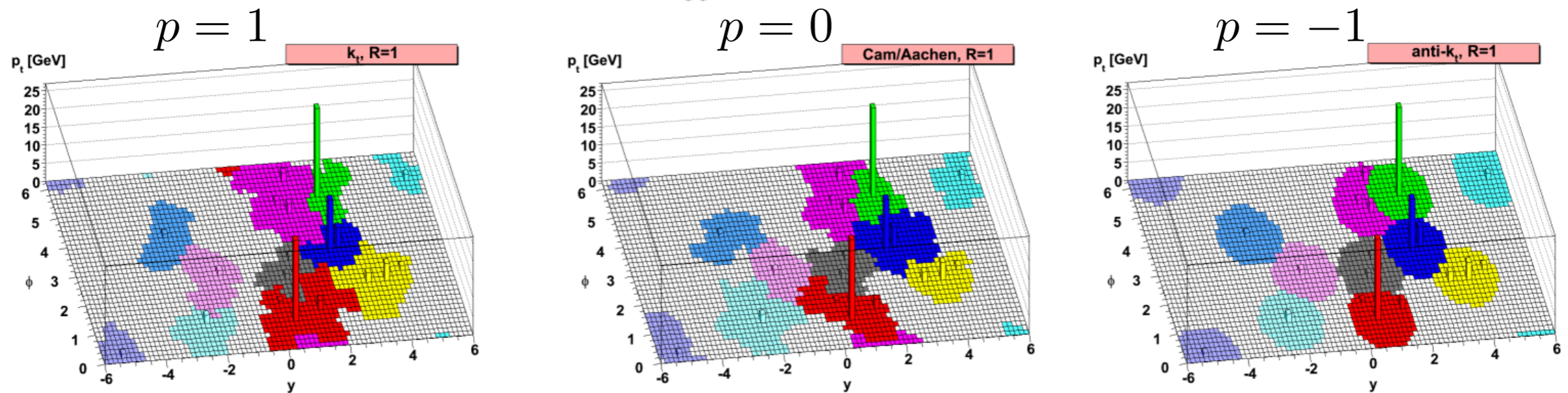


The anti- k_t jet clustering algorithm

Matteo Cacciari, Gavin P. Salam, Gregory Soyez, JHEP 04 (2008) 063

$$d_{ij} = \min(k_{ti}^{2p}, k_{tj}^{2p}) \frac{\Delta_{ij}^2}{R^2},$$

$$d_{iB} = k_{ti}^{2p},$$

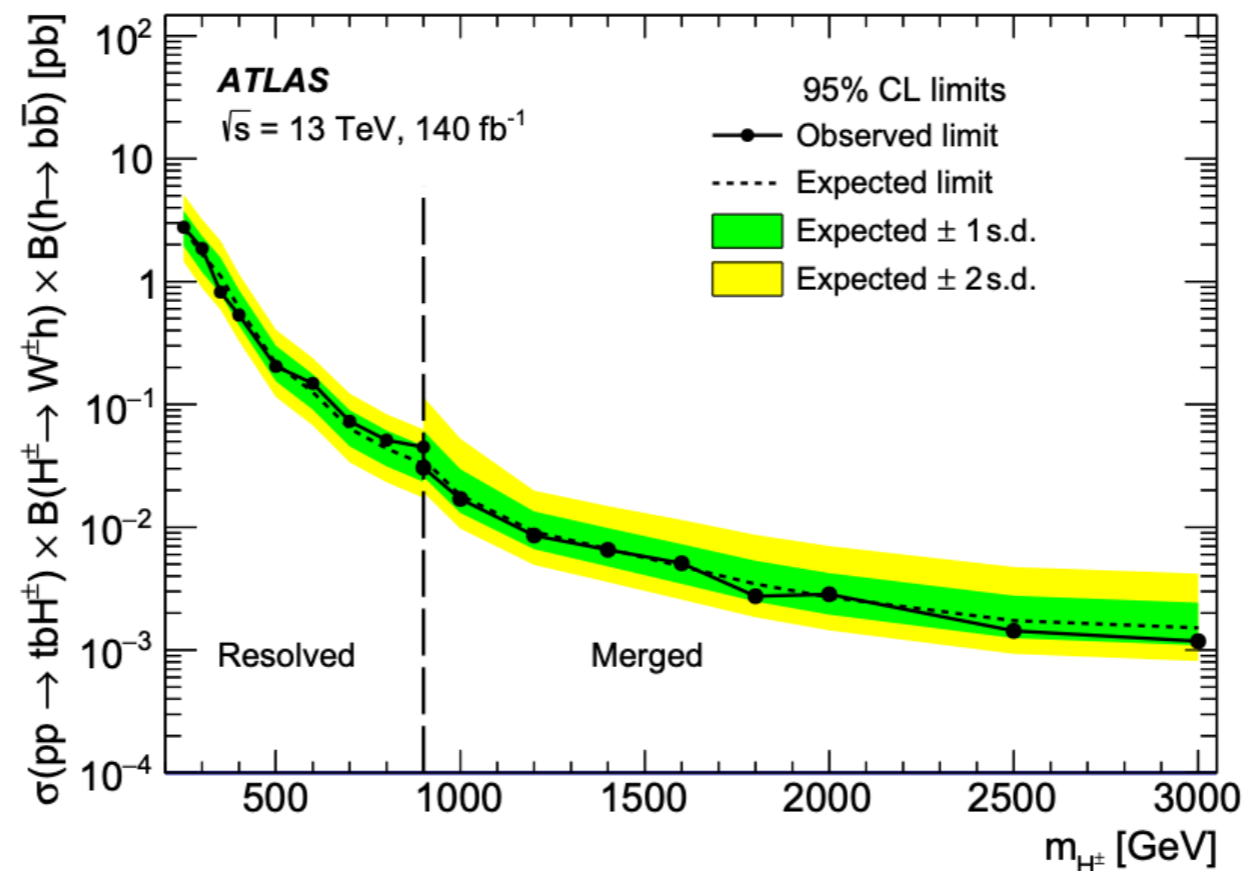


- LHC ‘incident’ 19 September 2008
- Startup delayed until 20 November 2009
- Anti- k_t adopted by all LHC experiments!
- k_t still useful for jet grooming and substructure ...

Search for a heavy charged Higgs boson decaying into a W boson and a Higgs boson in final states with leptons and b -jets in $\sqrt{s} = 13$ TeV pp collisions with the ATLAS detector

ATLAS, arXiv:2411.03969

“Large- R jets are used to reconstruct high-momentum Higgs or W -boson candidates, for which the hadronic decay products are emitted with small angular separation. These jets are built using a radius parameter of $R = 1.0$ Trimming [101] is used to minimise contributions from initial-state radiation, pile-up interactions or the underlying event. This is done by reclustering the constituents of the initial jet, using the k_t algorithm [102, 103], into subjets with a radius parameter of $R^{\text{sub}} = 0.2$ and then removing any subjet with a p_T less than 5% of the p_T of the parent jet [104]. The trimmed large- R jets are required to have $p_T > 250$ GeV and $|\eta| < 2.0$.”



Sudakov shoulder

The dipole formalism for the calculation of QCD jet cross sections at next-to-leading order

S. Catani, M.H. Seymour, PLB 378 (1996) 287

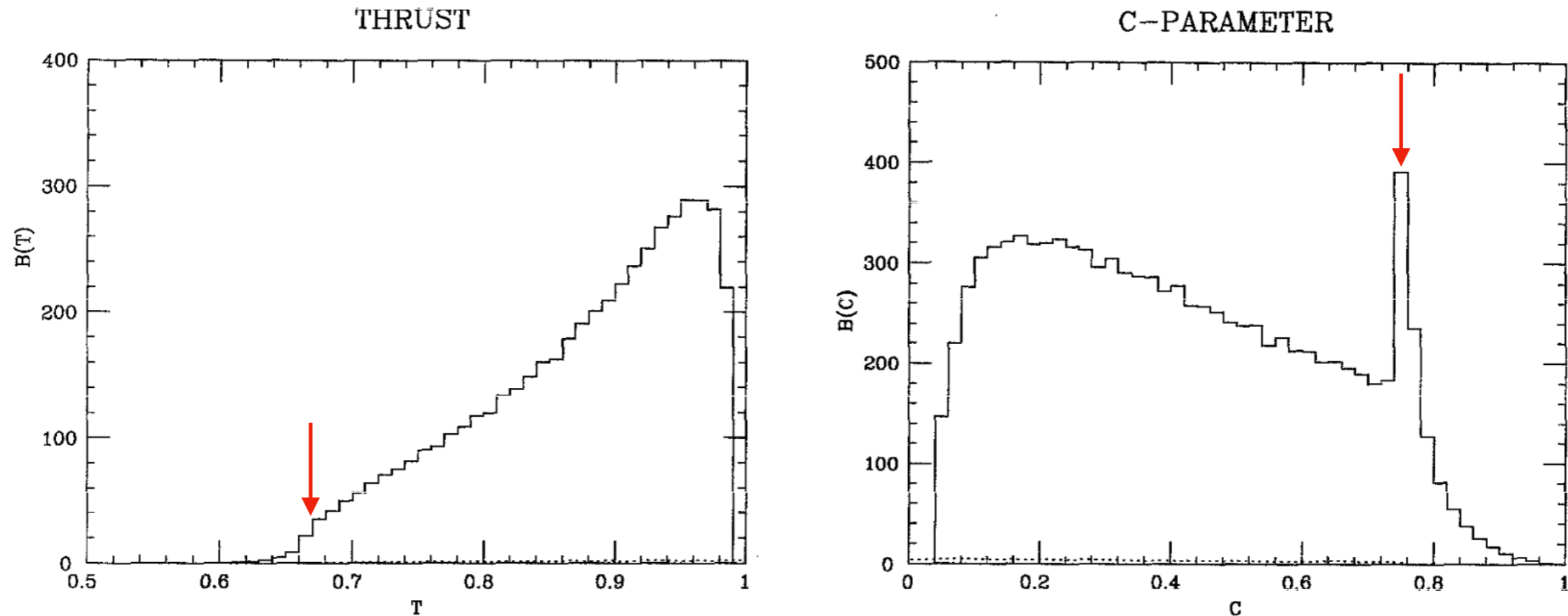
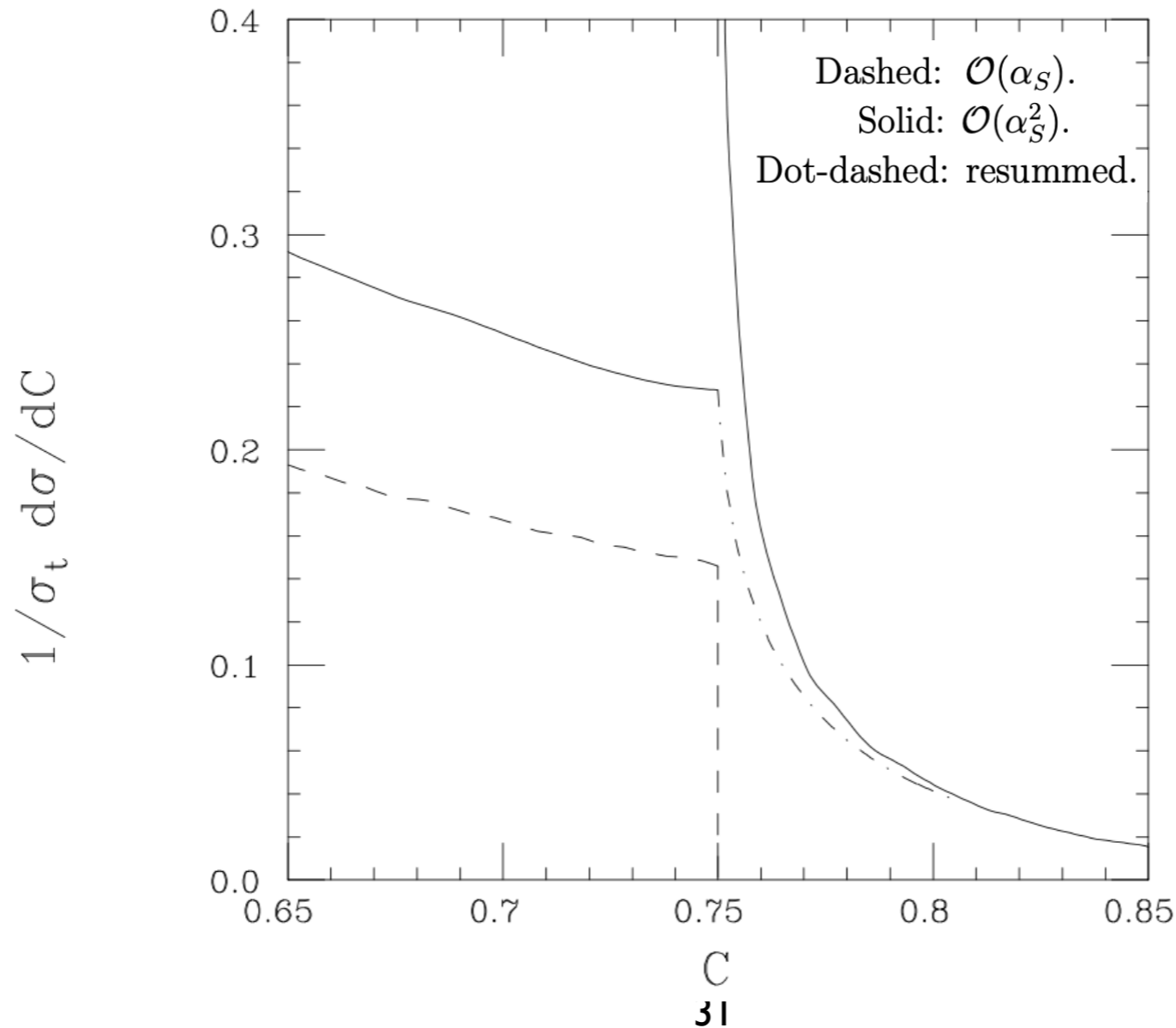


Fig. 1. Coefficient of $(\alpha_S/2\pi)^2$ for the thrust and C -parameter distributions. The dotted histograms show the size of the statistical errors.

Infrared Safe but Infinite: Soft-Gluon Divergences Inside the Physical Region

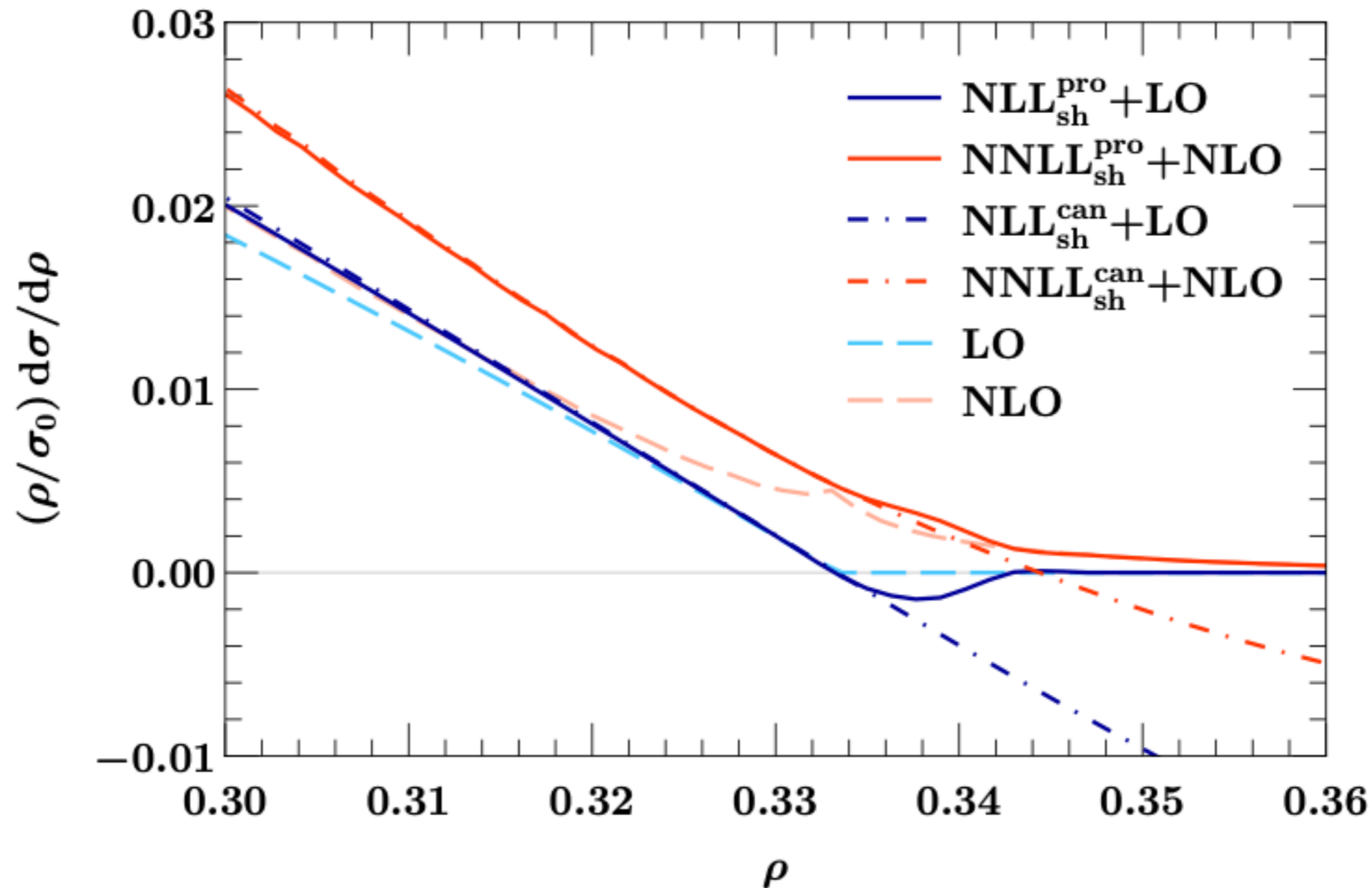
S. Catani, B.R. Webber, JHEP 10 (1997) 005

$$\hat{\sigma}_+^{(\infty)}(C) - \hat{\sigma}_-^{(\infty)}(C_0) = \exp\left\{-\frac{a}{2} \ln^2(C - C_0)\right\} \left[\hat{\sigma}_+^{(n_0)}(C_0) - \hat{\sigma}_-^{(n_0)}(C_0)\right]$$



NNLL resummation of Sudakov shoulder logarithms in the heavy jet mass distribution

Arindam Bhattacharya,^a Johannes K.L. Michel,^b Matthew D. Schwartz,^a
Iain W. Stewart^b and Xiaoyuan Zhang^a JHEP 11 (2023) 080



Jet shapes in hadron collisions: higher orders, resummation and hadronization

M.H. Seymour, NPB 513 (1998) 269

“ current cone-type jet definitions are not infrared safe for final states with more than three partons. Unless this situation is rectified by using improved definitions, hadron collider experiments will never be able to study the internal properties of jets with the quantitative accuracy already achieved in e^+e^- annihilation.”

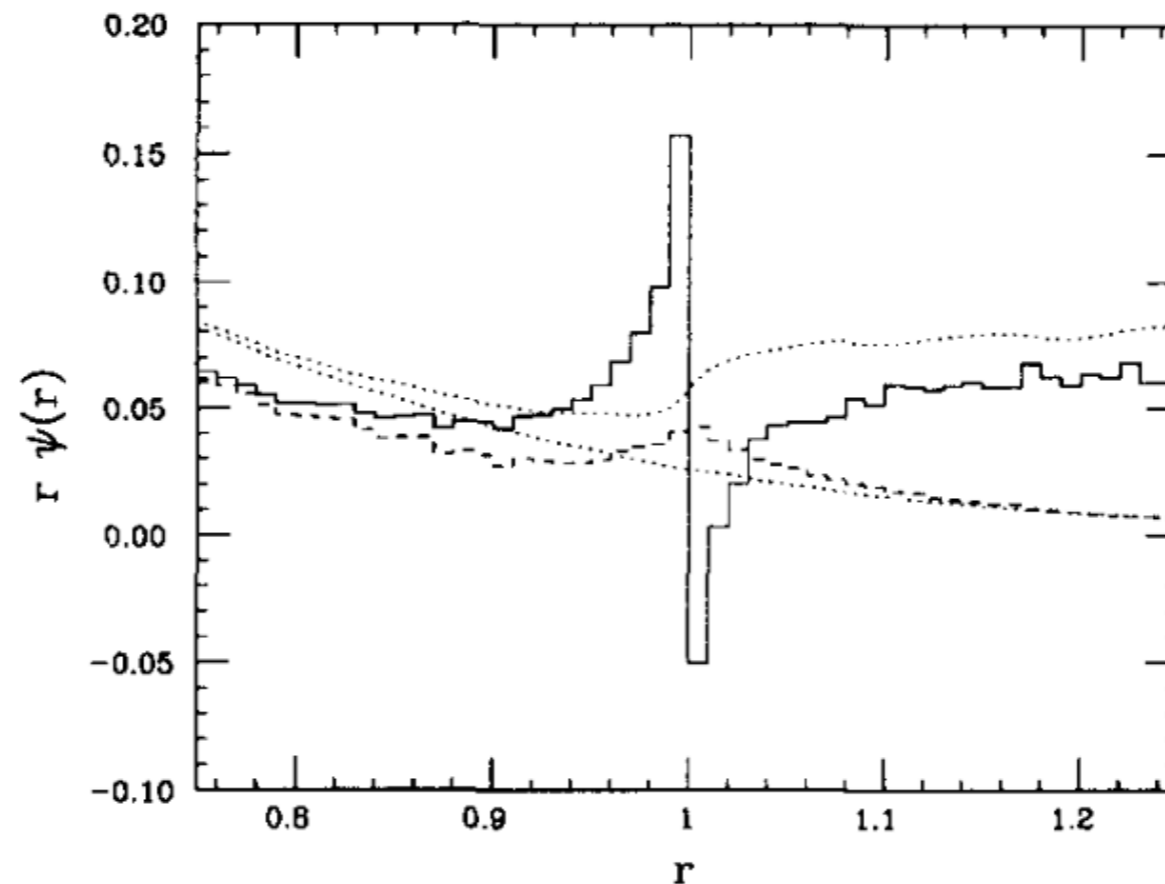
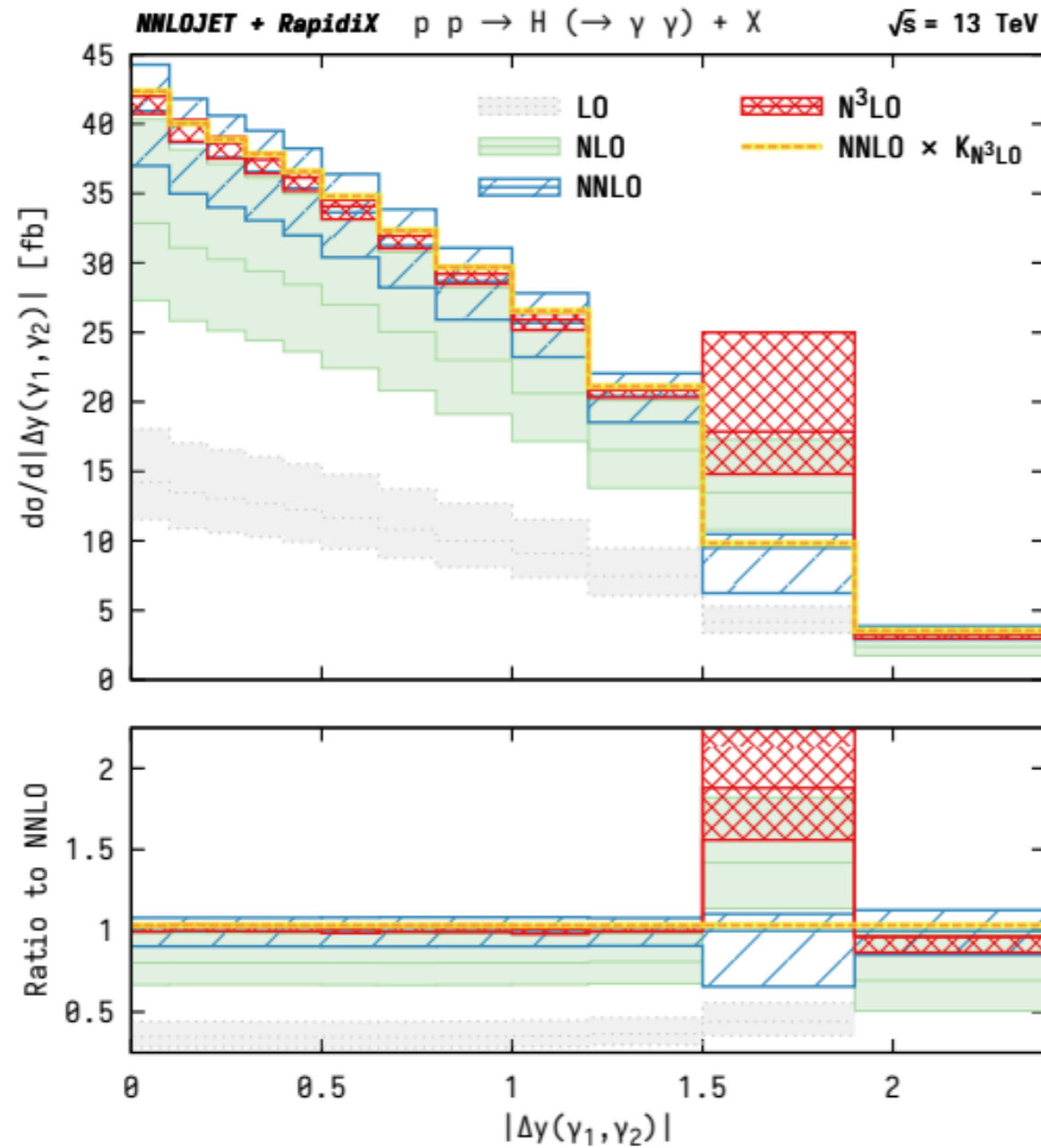


Fig. 11. The jet shape in the k_{\perp} jet algorithm at NLO (solid and dashed) and all orders (dotted). The solid and upper dotted curve use all particles in the event, the dashed and lower dotted curve use only those particles assigned to this jet.

Fully Differential Higgs Boson Production to Third Order in QCD

X. Chen^{1,2,3}, T. Gehrmann¹, E. W. N. Glover⁴, A. Huss⁵, B. Mistlberger⁶ and A. Pelloni⁷

PHYSICAL REVIEW LETTERS 127, 072002 (2021)



ATLAS cuts:

$$p_T^{\gamma_1} > 0.35 \times m_{\gamma\gamma}, \quad p_T^{\gamma_2} > 0.25 \times m_{\gamma\gamma},$$

$$|\eta^\gamma| < 2.37 \text{ excluding } 1.37 < |\eta^\gamma| < 1.52,$$

→ Sudakov shoulder at

$$2 \operatorname{arccosh}\left(\frac{M_H}{2 p_T^{\text{cut}}}\right) \equiv \Delta y_{\text{max}}|_{\text{LO}} \approx 1.8$$

CKKW

QCD Matrix Elements + Parton Showers

S. Catani^{a*}, F. Krauss^b, R. Kuhn^{c,d} and B.R. Webber^b, JHEP 11 (2001) 063

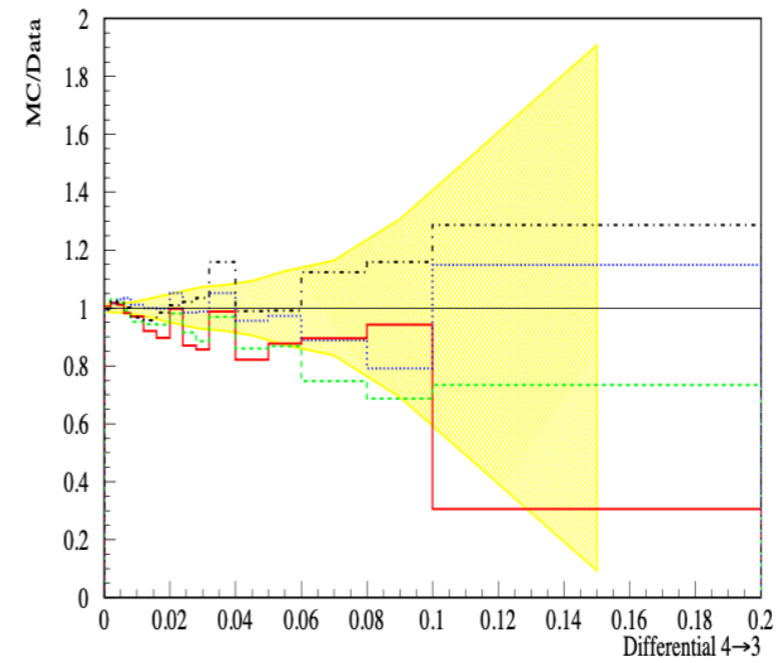
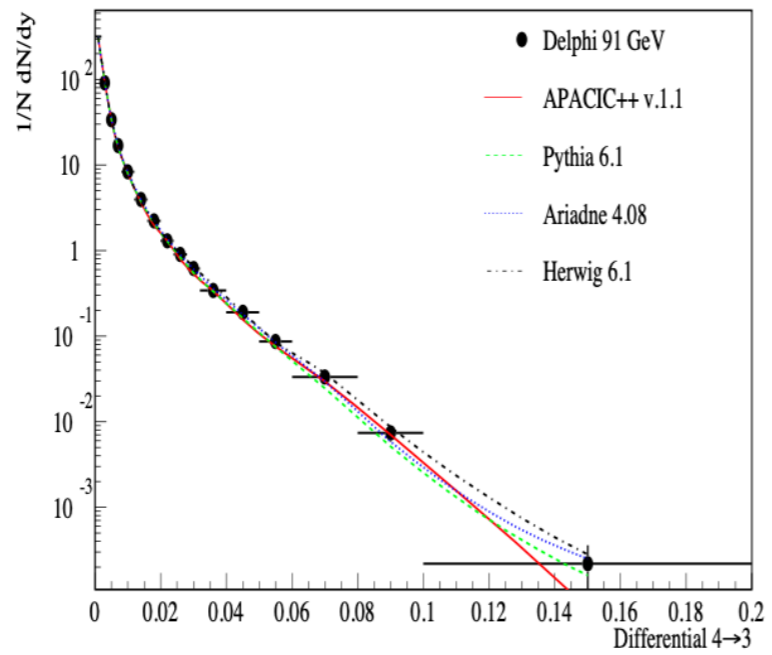
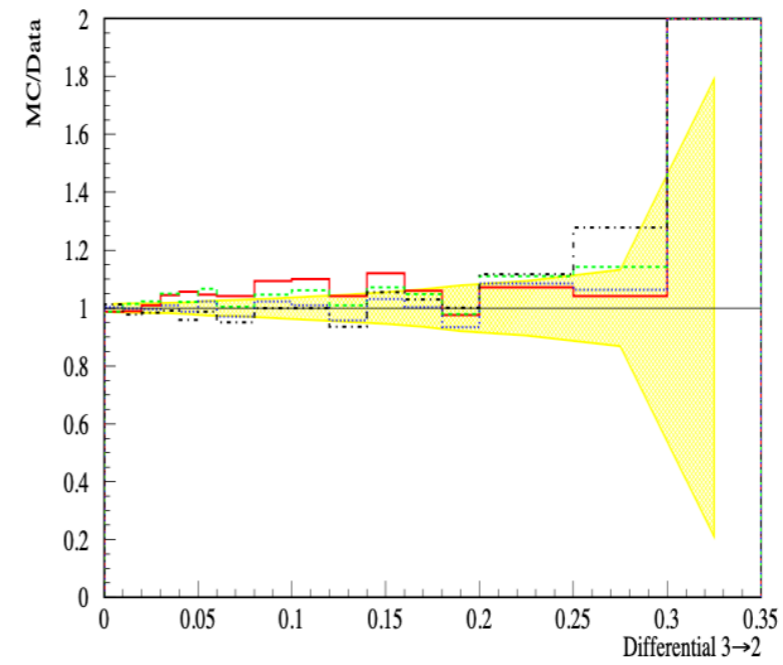
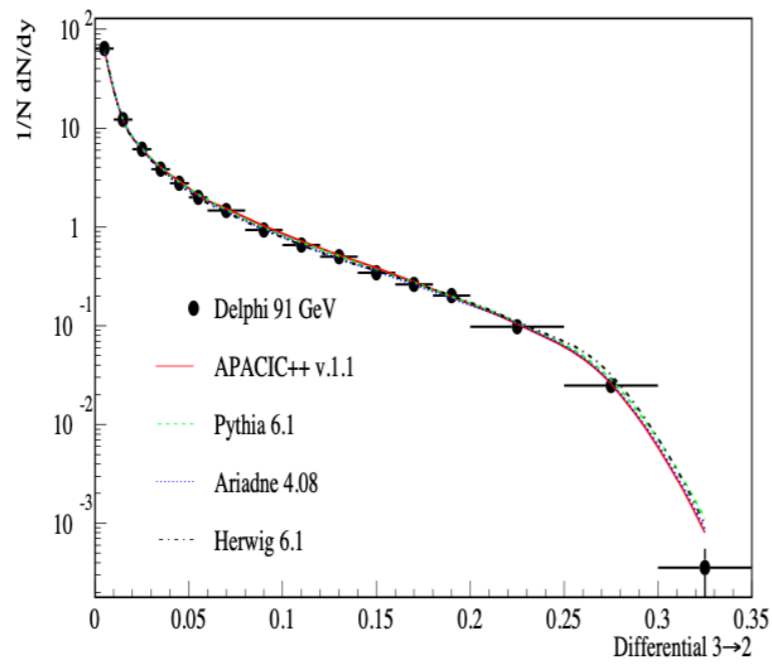
- Use fixed order x Sudakovs above scale Q_1
- Match to vetoed showers
- Veto cancels LL and NLL dependence on Q_1

$$R_n^{(q)}(y_{\text{ini}} = Q_1^2/Q^2) = \frac{1}{n!} \left(\frac{\partial}{\partial u} \right)^n \phi_q(Q_1, Q; u_q = u_g = u)|_{u=0}$$

$$\phi_q(Q_1, Q; u_q, u_g) = u_q \exp \left\{ \int_{Q_1}^Q dq \Gamma_q(q, Q) [\phi_g(Q_1, q; u_q, u_g) - 1] \right\}$$

$$\phi_i(Q_1, Q; \tilde{\phi}_q, \tilde{\phi}_g) = \phi_i(Q_0, Q; u_q, u_g)$$

$$\rightarrow \tilde{\phi}_q(Q_0, Q_1, Q; u_q, u_g) = u_q \exp \left\{ \int_{Q_0}^{Q_1} dq \Gamma_q(q, Q) [\phi_g(Q_0, q; u_q, u_g) - 1] \right\}$$



● LO matching results were not that great!

CKKW in SHERPA

Matrix Elements and Parton Showers in Hadronic Interactions
Frank Krauss, JHEP 08 (2002) 015

**NLO QCD matrix elements + parton showers
in $e^+e^- \rightarrow$ hadrons**

Thomas Gehrmann¹, Stefan Höche², Frank Krauss³, Marek Schönherr³, Frank Siegert⁴

JHEP 01 (2013) 144

**QCD matrix elements + parton showers
The NLO case**

Stefan Höche¹, Frank Krauss², Marek Schönherr², Frank Siegert³

JHEP 04 (2013) 027

Measurement of off-shell Higgs boson production in the $H^* \rightarrow ZZ \rightarrow 4\ell$ decay channel using a neural simulation-based inference technique in 13 TeV pp collisions with the ATLAS detector

CERN-EP-2024-298
December 3, 2024

Sample	ME generator	PS	Higher-order correction
$gg \rightarrow ZZ$	SHERPA 2.2.2 (LO [1j])	SHERPA 2.2.2	NLO QCD (m_{ZZ} dependent) [59] Approx. N3LO QCD (global) [64]
EW $q\bar{q} \rightarrow ZZ + 2j$	MG5_AMC@NLO 2.3.3	PYTHIA 8.244	-
$q\bar{q} \rightarrow ZZ$	SHERPA 2.2.2 (NLO [1j], LO [3j])	SHERPA 2.2.2	NLO EW (m_{ZZ} dependent) [69, 70]
WWZ, WZZ, ZZZ	SHERPA 2.2.2	SHERPA 2.2.2	-
$t\bar{t}Z$	MG5_AMC@NLO 2.3.3	PYTHIA 8.210	NLO QCD + NLO EW (global) [71]

Jet merging uncertainties are evaluated by varying the matching scale (based on the Catani-Krauss-Kuhn-Webber CKKW prescription [98]) for the processes simulated with the SHERPA generator. Parton-shower uncertainties are evaluated by varying the SHERPA showering scheme [58].

The largest contributions to the measurement uncertainty are the statistical uncertainty on the data, the theoretical modeling uncertainties, and uncertainties on the jet energy scale and resolution. The contribution of MC statistical uncertainty to the total uncertainty is less than 0.01. The observed (expected) value of $\mu_{\text{off-shell}}$ at 68% CL is:

$$\mu_{\text{off-shell}} = 0.87^{+0.75}_{-0.54} \quad (1.00^{+1.04}_{-0.95}).$$

Merging meets matching in MC@NLO

R. Frederix, S. Frixione, JHEP 12 (2012) 061

FxFx \rightarrow MadGraph5_aMC@NLO

The automated computation of tree-level and next-to-leading order differential cross sections, and their matching to parton shower simulations

J. Alwall^a, R. Frederix^b, S. Frixione^b, V. Hirschi^c, F. Maltoni^d, O. Mattelaer^d, H.-S. Shao^e, T. Stelzer^f, P. Torrielli^g, M. Zaro^{hi}, JHEP 07 (2014) 079

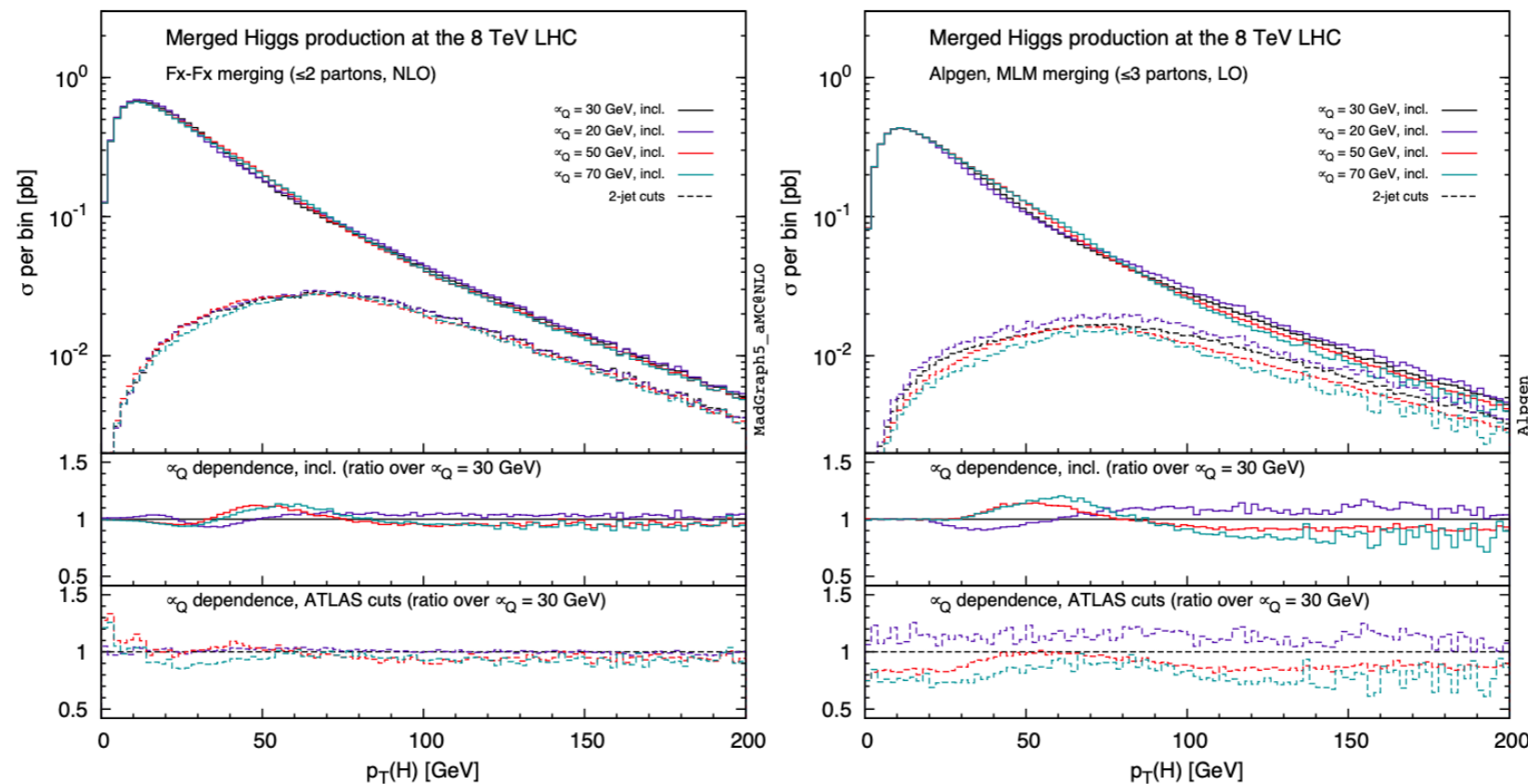


Figure 14: Higgs transverse momentum in single-Higgs production (gluon-gluon fusion in HEFT), as predicted by FxFx (left panel) and ALPGEN (right panel), for various choices of the merging scale μ_Q .

Final Remarks

- All of us who worked with Stefano benefited immeasurably
- His ideas were foundational for many tests and applications of QCD
- They will continue to be used and developed as long as particle physics is done

**Thanks for your
attention!**

Backup

$$R_n^H = (aL^2)^{n-2} (A + B/L + C/L^2)$$

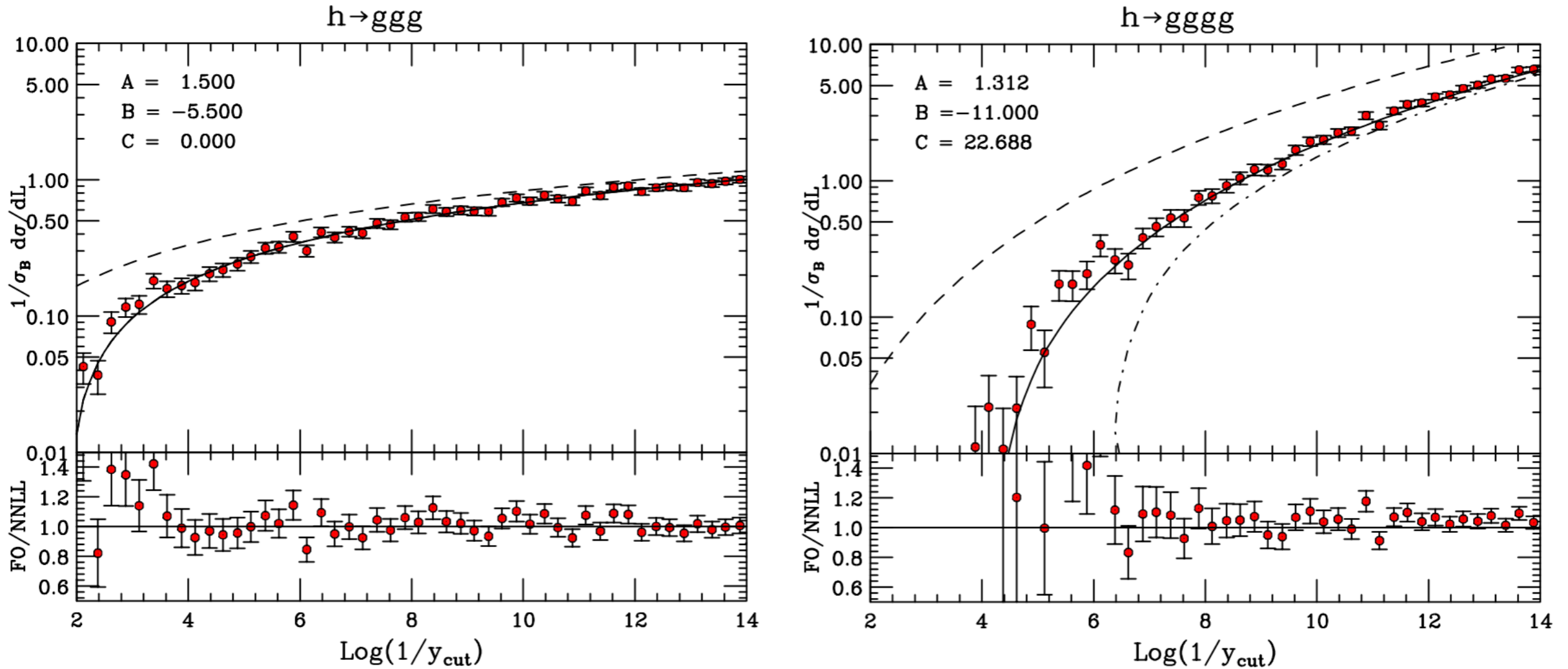


Figure 1: Differential distribution of $L = \ln(1/y_{\text{cut}})$ in $h \rightarrow 3$ and 4 gluons. Points are MadGraph data using leading-order exact matrix elements. Dashed, dot-dashed and solid curves show the leading-log, NLL and NNLL results, respectively.

(BRW, unpublished)

Average number of jets in e^+e^- annihilation

S. Catani, Yu.L. Dokshitzer, F. Fiorani, B.R. Webber, NPB 377 (1992) 445

$$\mathcal{N}_q^c(Q_0, Q) = \delta_q^c + \int_{Q_0}^Q \frac{dq}{q} \frac{\alpha_s(q)}{\pi} 2C_F \left(\ln \frac{Q}{q} - \frac{3}{4} \right) \mathcal{N}_g^c(Q_0, q),$$

$$\mathcal{N}_g^c(Q_0, Q) = \delta_g^c + \int_{Q_0}^Q \frac{dq}{q} \frac{\alpha_s(q)}{\pi} \left\{ \left[2C_A \left(\ln \frac{Q}{q} - \frac{11}{12} \right) - \frac{n_f}{3} \right] \mathcal{N}_g^c(Q_0, q) + \frac{2n_f}{3} \mathcal{N}_q^c(Q_0, q) \right\}.$$

$$\begin{aligned} \mathcal{N}_{ee} = & 2 + C_F \frac{\alpha_s}{2\pi} \left[\ln^2 y + 3 \ln y + O(1) \right] \\ & + C_F \left(\frac{\alpha_s}{2\pi} \right)^2 \left[\frac{1}{12} C_A \ln^4 y - \frac{1}{9} (C_A - n_f) \ln^3 y + O(\ln^2 y) \right] \\ & + C_F \left(\frac{\alpha_s}{2\pi} \right)^3 \left[\frac{1}{360} C_A^2 \ln^6 y - \left(\frac{7}{72} C_A^2 - \frac{1}{30} C_A n_f + \frac{1}{90} C_F n_f \right) \ln^5 y + O(\ln^4 y) \right] + \dots \end{aligned}$$

- **NDLA not NLLA: not so good for precision**